No. 2A-2 $LiTaO_3$, Lithium tantalate
(M = 235.887)

1a Ferroelectricity in $LiTaO_3$ was discovered by Matthias and Remeika in 1949. 49Mat

b

phase	II	I
state	F	P
crystal system	trigonal	trigonal
space group	$R3c - C_{3v}^6$ [a])	$R\bar{3}c - D_{3d}^6$ [b])
Θ_f [°C]	665(5)	

[a])54Meg
[b])67Abr1
64Raz

P_s || [001] of hexagonal unit cell. 54Meg
T_{melt} = 1650 °C. 65Bal
$\rho_X = 7.4564 \cdot 10^3$ kg m^{-3}. 67Abr1
See Fig. 2A-2-001.
Phase relation: Fig. 2A-2-002.
Raman spectra show an amorphous state above 33.2 GPa: see 94Lin
Vitreous state: see 77Gla

2a Crystal growth: Czochralski method. 65Bal, 65Fed
Flux-grown crystals: see 89YeZ
Producing shaped single crystals by Stepanov (EFG) method (review paper): see 86Red
Ceramics obtained from powders prepared by sol-gel method: see 88Rav
Epitaxial growth of thin films on sapphire substrates by RF magnetron sputtering: see 92Sai
Synthesis of whiskers from metal alkoxide derived gels: see 93Dei
Epitaxial growth of thin films on sapphire substrate by excimer laser ablation method: see 93Shi
Epitaxial thin film growth by metalorganic chemical vapor deposition (CVD): see 93Xie
Chemical preparation of spherical particle powder: see 90Jea1
Epitaxial growth on sapphire c-substrate by RF magnetron sputtering: see 91Sai
Sol-gel derived thin films: see 90Jea2
Epitaxial nonlinear optical films on GaAs: see 93Hun
Proton-exchange by pyrophosphoric acid: see 92Yam1
Proton-exchange in melts of acids and acidic salts: see 89Gan
Proton-exchange with controlled acidity (review paper): see 90Gan

3a a_{hex} = 5.15428 Å, c_{hex} = 13.78351 Å and a_{rh} = 5.4740 Å, α_{rh} = 56°10.5' at 25 °C. 67Abr1
Fig. 2A-2-001.

b Z = 4 in hexagonal unit cell. 67Abr1
Crystal structure: Tables 2A-2-001...003; Fig. 2A-2-003, Fig. 2A-2-004.

4 Thermal expansion: $\alpha_a^{(1)} = 0.161 \cdot 10^{-4}$ °C^{-1}, $\alpha_a^{(2)} = 0.070 \cdot 10^{-7}$ °C^{-2}; 71Smi
$\alpha_c^{(1)} = 0.041 \cdot 10^{-4}$ °C^{-1}, $\alpha_c^{(2)} = -0.100 \cdot 10^{-7}$ °C^{-2}, where
$\Delta a/a = \alpha_a^{(1)} (T - T_0) + \alpha_a^{(2)} (T - T_0)^2$,
$\Delta c/c = \alpha_c^{(1)} (T - T_0) + \alpha_c^{(2)} (T - T_0)^2$, with T_0 = 25 °C.
Fig. 2A-2-005.

5a Dielectric constant: Table 2A-2-004, Table 2A-2-005;
Figs. 2A-2-006...2A-2-028;
see also Fig. 2A-1-026, Fig. 2A-1-027 in No. 2A-1.

	Vitreous specimens prepared by roller quenching: see	77Gla
	Curie-Weiss constant: $C = 1.5 \cdot 10^5$ K.	69Yam
c	Spontaneous polarization: $P_s = 0.50$ Cm^{-2}.	68Wem
	Fig. 2A-2-029, Fig. 2A-2-030.	
	Point defects and singularities of low temperature behavior of P_s: see	91Nov
d	Pyroelectricity $p_3 = -17.6 \cdot 10^{-5}$ CK^{-1}m^{-2} (primary effect: $-17.8 \cdot 10^{-5}$ CK^{-1}m^{-2}, secondary effect: $+0.200 \cdot 10^{-5}$ CK^{-1}m^{-2}) at RT;	80Bha
	see also	75Bee
	Fig. 2A-2-031, Fig. 2A-2-032.	
	Pyroelectric properties of various $LiTaO_3$ related ceramics: see	90InH
	Data for calculating figure of merits: see	75Bee
	Point defects and singularities of low temperature behavior of p: see	91Nov
6a	Heat capacity: $C_p = 100$ J K^{-1} mol^{-1} at 25 °C.	75Bee
	Fig. 2A-2-033.	
7a	Piezoelectricity: Fig. 2A-2-034; see also Table 2A-2-004 and Table 2A-2-006.	
	Pressure dependence of piezoelectric polarization: see	76Gra
8a	Elastic compliance and stiffness: see Table 2A-2-004 in 5a, and Table-2A-006 in 7a; Figs. 2A-2-035...2A-2-040.	
	Acoustic properties: see Table 2A-1-012 in No. 2A-1.	
	Temperature dependence of plate resonators: see	76Bur
	Surface acoustic wave: Table 2A-2-007.	
	Temperature dependence: see	72Sch
	Effect of film loading: see	75Par
	Surface acoustic wave: The X-cut 112° rotated Y propagation mode has a low bulk spurious response level and a low temperature coefficient of propagation delay time as well as a high coupling coefficient.	77Hir
	Table 2A-2-008; Fig. 2A-2-041, Fig. 2A-2-042.	
	Temperature coefficient adjustment of propagation delay time by SiO_2 coating, see	81Ina
	Internal friction: Fig. 2A-2-043.	
	Quantitative evaluation of elastic properties by acoustic microscopy: see	91Kus
9a	Refractive index: Table 2A-2-009; Fig. 2A-2-044, Fig. 2A-2-045.	
	Birefringence: Fig. 2A-2-046.	
	Light transmission: Fig. 2A-2-047.	
	Reflection: Fig. 2A-2-048; see also Fig. 2A-2-024 in 5a.	
	Absorption: Fig. 2A-2-045; see also Fig. 2A-2-025 in 5a, Fig. 2A-1-087 in No. 2A-1.	
	Anomalous refractive index change and recovery of electrooptic coefficient g_{33} in proton-exchanged optical waveguides after annealing: see	92Yuh
b	Electrooptic effect: Table 2A-2-010.	
	Quadratic electrooptic constant:	
	$M_{13}^{\mathbf{T}} = 0.013(3)$ m^{4}C^{-2}, $M_{33}^{\mathbf{T}} = 0.061(1)$ m^{4}C^{-2} ($\lambda = 644$ nm).	68Iwa
	Electrooptical properties in the temperature range 15...950 K: see	92Sha
c	Piezooptic effect: Table 2A-2-011, Table 2A-2-012.	
d	Faraday effect: see Fig. 2A-1-091 in No. 2A-1.	
e	Nonlinear optical property:	
	$d_{22} / \left\lvert d_{36}^{\mathrm{KDP}} \right\rvert = 4.4$, $d_{31} / \left\lvert d_{36}^{\mathrm{KDP}} \right\rvert = d_{15} / \left\lvert d_{36}^{\mathrm{KDP}} \right\rvert = -2.7$, $d_{33} / \left\lvert d_{36}^{\mathrm{KDP}} \right\rvert = -41$ at RT	69Bec,
	for $\lambda = 1.058$ μm.	70Mil
	Nonlinear millimeter wave susceptibility:	

	$d_{33} = 18.62 \cdot 10^{-9}$ mV^{-1} for λ = 857 μm (f = 35 GHz).	83Ahn
	Nonlinear optical properties of proton-exchanged waveguide: see	94Ahl1
	Blue light generation in a waveguide by quasi-phase-matched second harmonic generation: see	91Miz1
	Characteristics of periodically domain-inverted (by proton-exchange) waveguides for second harmonic generation: see	91Yam
10a	Raman scattering: Table 2A-2-013; Figs. 2A-2-049...2A-2-058; see also	84Men, 87Yan, 87Vor
	New low frequency Raman modes from proton-exchanged crystals: see	95WuX
	Raman scattering in Nd-doped crystal: see	94WuX1
	Raman spectra showed that $LiTaO_3$ becomes amorphous above 33.2 GPa: see	94Lin
	Raman scattering under high pressure: see	86Jay
	Hyper Raman scattering: Fig. 2A-2-059, Fig. 2A-2-060.	
	Stimulated Raman scattering by femtosecond laser pulses: Fig. 2A-2-061, Fig. 2A-2-062.	
	Observation of THz phonon-polariton beats by femtosecond laser pulses: see	92Bak
	Brillouin scattering: Table 2A-2-014.	
	Rayleigh scattering: Fig. 2A-2-063, see also	86Zha
11	Resistivity: $\rho = 3.6 \cdot 10^8$ Ωm at 25 °C ,1 kHz.	75Bee
	Conductivity: Fig. 2A-2-064, Fig. 2A-2-065; see also Fig. 2A-2-007 in 5a.	
	Bulk and surface resistivity: see	94Len
	Humidity dependence of surface resistance: see	92Mae
	Luminescence from Cr^{3+} ion: see	69Gla
	Exoelectron emission: see	80Ros
	Seebeck effect: Fig. 2A-2-066.	
	Photovoltaic effect: Fig. 2A-2-067.	
13a	NMR: e^2qQ/h = 77.6(5) kHz for ^{7}Li,	68Pet
	e^2qQ/h = 60.2(3) kHz for ^{8}Li.	77Dub
	Fig. 2A-2-073.	
	NMR of Li: see also	85Sen
b	ESR: Table 2A-2-015, Table 2A-2-016.	
	ESR of Ti^{3+}: $g_\parallel$ = 1.948(3), $g_\perp$ = 1.827(3).	94Thi
	ENDOR of Fe^{3+}: g = 1.995(2) (nearly isotropic). $3B_2^0$ = 9900(100) MHz.	89Sot
	ESR spin Hamiltonian parameters of Co^{2+}: $g_\parallel$ = 2.38, $g_\perp$ = 5.02, $A_\parallel \approx 0$, $A_\perp = 133 \cdot 10^{-2}$ m^{-1}.	87Don
c	Mössbauer effect (^{57}Fe): $e^2qQ(7/2)$ = 46.4(2) mm s^{-1} = 9.59(4)·10^{-7} eV, $\delta = -17.95(10)$ mm s^{-1}.	78Wor
	Figs. 2A-2-069...2A-2-072.	
	Mössbauer effect of ^{57}Co: see	90Leu, 90And
14	Small ionic displacements under ac electric fields applied along the c-axis have been observed by X-ray diffraction.	82Fuj
	EXAFS of Co and Fe doped crystals: see	91Cat1
15a	Domain structure: see	66Lev
	Observation of 180° domain walls by high resolution electron microscopy: see	82Lin
	Poling method with an aid of electron beams: see	86Hay

	Domain thickness: Fig. 2A-2-073.	
	Domain inversion using proton-exchange followed by heat treatment: see	94Miz1
	Periodic domain inversion by electron beam scanning: see	94Gup
	Fabrication of periodically domain-inverted structure by proton-exchange and heat treatment: see	91Miz2
	Characteristics of periodically domain-inverted (by proton-exchange) waveguides for second harmonic generation: see	91Yam
	Fabrication of periodically domain-inverted structure by proton-exchange with pyrophosphoric acid: see	92Miz1
	Quasi-phase-matched second-harmonic generation using a periodically domain-inverted waveguide: see	92Miz2
	Fabrication of periodically inverted domain structures using proton-exchange: see	92Mak
16	Investigation of the effect of internal heat transfer on growth behavior in Czochralski crystal growth process: see	94Oka
	Direct bonding of single crystals: see	94Tom
	Fabrication of periodically inverted domain structures using proton-exchange: see	92Mak
	Vapor diffused Zn-doped optical waveguides: see	88Yoo
	Fabrication of alternating $LiNbO_3$/$LiTaO_3$ layers: see	87Kan
	Surface layer: surface breakdown by laser pulses: see	72Zve
	Electron spectroscopic studies of surfaces: see	81Rit
	Etchant: mixture of hydrofluoric acid and nitric acid at its boiling point: see	66Lev
	Optical waveguide: many fabrication techniques have been reported;	
	by out-diffusion, see	73Kam
	by in-diffusion, see	74Ham, 74Nod
	by sputtering , see	73Gia
	a review paper, see	75Tie
	Formation of ion exchanged $LiTaO_3$:Cu waveguides: see	91Bob
	Blue light generation by frequency doubling of a laser diode in a periodically domain-inverted waveguide: see	92Yam2
	Quasi-phase-matched waveguides fabricated by domain inversion with proton-exchange and heat treatment technique: see	92Yam3
	Quasi-phase-matched second-harmonic generation in a waveguide: see	94Miz2
	Blue light generation in a waveguide by quasi-phase-matched second harmonic generation: see	91Miz1
	Quasi-phase-matched second-harmonic generation using a periodically domain-inverted waveguide: see	92Miz2
	Optical damage: change of refractive indices occurs in the region illuminated by laser beams: see	66Ash
	Optical waveguide fabrication by proton-exchange: see	83Spi
	Photoinduced light scattering: see	94WuX2
	Photorefractive effects in proton-exchanged optical waveguides: see	92McW
	X-ray topographic study: see	82Yas1
	$^{181}Hf \rightarrow {}^{181}Ta$ perturbed-angular correlation spectroscopy: Fig. 2A-2-074.	

Table 2A-2-001. $LiTaO_3$. Fractional atomic coordinates and anisotropic temperature parameters at various temperatures refined by the method of least squares fitting in space group R3c [73Abr]. b_{ij} is defined by Eq. (b) in Introduction.

Parameter	297 K	760 K	820 K	885 K	940 K
z(Li)	0.2790(17)	0.2812(26)	0.2818(19)	0.2765(15)	0.2761(14)
b_{11}(Li)	0.0106(61)	0.0349(101)	0.0205(56)	0.0354(68)	0.0578(82)
b_{33}(Li)	0.0043(10)	0.0071(21)	0.0093(18)	0.0047(12)	0.0077(18)
b_{11}(Ta)	0.0055(17)	0.0062(17)	0.0085(14)	0.0118(16)	0.0195(13)
b_{33}(Ta)	0.0003(1)	0.0007(2)	0.0009(1)	0.0011(1)	0.0017(1)
x(O)	0.0501(5)	–0.0543(5)	0.0547(4)	0.0557(5)	0.0540(5)
y(O)	0.3436(3)	0.3396(5)	0.3394(4)	0.3381(5)	0.3345(11)
z(O)	0.0687(3)	0.0756(3)	0.0786(2)	0.0835(3)	0.0817(5)
b_{11}(O)	0.0056(12)	0.0126(12)	0.0162(12)	0.0206(19)	0.0159(15)
b_{22}(O)	0.0038(14)	0.0099(11)	0.0109(10)	0.0118(11)	0.0149(8)
b_{33}(O)	0.0011(2)	0.0014(2)	0.0020(2)	0.0021(1)	0.0027(1)
b_{12}(O)	0.0019(12)	0.0054(10)	0.0069(9)	0.0105(15)	0.0052(15)
b_{13}(O)	–0.0004(4)	–0.0010(4)	–0.0008(3)	–0.0021(4)	–0.0018(6)
b_{23}(O)	–0.0007(2)	–0.0021(2)	–0.0022(2)	–0.0031(1)	–0.0032(1)
R	0.0335	0.0526	0.0431	0.0486	0.0320

Table 2A-2-002. $LiTaO_3$. Fractional atomic coordinates and anisotropic temperature parameters at 885 K and 940 K in centrosymmetric space group $R\bar{3}c$ (a) and $R\bar{3}$ (b) [73Abr]. b_{ij} is defined by Eq. (b) in Introduction.

Parameter	885 K (a)	940 K (a)	940 K (b)
z(Li)	0.2833(30)	0.2772(15)	0.2501(46)
b_{11}(Li)	0.0820(209)	0.0535(84)	0.0551(105)
b_{33}(Li)	0.0063(14)	0.0075(17)	0.0270(42)
b_{11}(Ta)	0.0151(23)	0.0198(14)	0.0200(21)
b_{33}(Ta)	0.0009(2)	0.0017(1)	0.0016(2)
x(O)	0.0531(5)	0.0531(2)	0.0534(4)
y(O)	1/3	1/3	0.3339(5)
z(O)	1/12	1/12	0.0834(2)
b_{11}(O)	0.0200(22)	0.0271(12)	0.0182(10)
b_{22}(O)	0.0100(16)	0.0158(9)	0.0152(10)
b_{33}(O)	0.0021(2)	0.0027(1)	0.0028(1)
b_{12}(O)	$b_{22}/2$	$b_{22}/2$	0.0075(7)
b_{13}(O)	$b_{23}/2$	$b_{23}/2$	–0.0016(3)
b_{23}(O)	–0.0030(2)	–0.0033(2)	–0.0032(2)
R	0.0544	0.0339	0.0349

Table 2A-2-003. $LiTaO_3$. Interatomic distances and angles at 24 °C [67Abr1, 67Abr2].

Distance [a])	[Å]	Distance [a])	[Å]	Distance [b])	[Å]	Distance [b])	[Å]
Ta–Ta	3.759(0)	O–O	2.734(25)	Ta–Ta	3.759(0)	O–O	2.724(3)
Li–Li	3.759(0)		2.792(6)	Li–Li	3.759(0)		2.791(1)
Ta–O	1.891(10)		2.812(7)	Ta–O	1.908(3)		2.826(1)
	2.070(10)		2.823(22)		2.073(3)		2.870(3)
			3.064(9)				3.039(2)
Ta–Li	3.003(40)		3.425(18)	Ta–Li	3.046(23)		3.378(4)
	3.058(9)				3.068(6)		
	3.374(19)	Li–O	2.076(16)		3.354(11)	Li–O	2.041(7)
	3.888(40)		2.293(32)		3.845(23)		2.312(16)
Angle [a])	[°]	Angle [a])	[°]	Angle [b])	[°]	Angle [b])	[°]
O–Ta–O	82.7(5)	O–Li–O	73.2(12)	O–Ta–O	82.2(1)	O–Li–O	72.2(6)
	89.5(2)		79.2(5)		88.9(1)		79.5(2)
	90.4(2)		88.9(6)		90.4(1)		88.3(3)
	96.6(4)		111.1(10)		97.5(2)		111.9(5)
Average	89.8	Average	88.1	Average	89.8	Average	87.9

[a]) X-ray diffraction [67Abr1]. [b]) Neutron diffraction [67Abr2].

Table 2A-2-004. $LiTaO_3$. Elastic, piezoelectric, dielectric constants and their temperature coefficients. For definition of $a^{(1)}$, $a^{(2)}$, see original papers [71Smi, 67War1, 69Yam].

	Absolute quantities			Normalized temperature coefficients [71Smi]	
	[71Smi]	[67War1]	[69Yam]	$a^{(1)}$	$a^{(2)}$
Elastic stiffness	$[\cdot 10^{11}\,Nm^{-2}]$	$[\cdot 10^{11}\,Nm^{-2}]$	$[\cdot 10^{11}\,Nm^{-2}]$	$[\cdot 10^{-4}\,K^{-1}]$	$[\cdot 10^{-7}\,K^{-2}]$
c_{11}^{E}	2.298	2.33	2.28	–1.03	0.77
c_{12}^{E}	0.440	0.47	0.31	–3.41	–1.18
c_{13}^{E}	0.812	0.80	0.74	–0.50	6.00
c_{14}^{E}	–0.104	–0.11	–0.12	6.67	16.7
c_{33}^{E}	2.798	2.75	2.71	–0.96	–3.21
c_{44}^{E}	0.968	0.94	0.96	–0.43	1.67
c_{66}^{E}	0.929	0.93	0.98	–0.47	1.24
Elastic compliances	$[\cdot 10^{-12}\,m^2N^{-1}]$	$[\cdot 10^{-12}\,m^2N^{-1}]$	$[\cdot 10^{-12}\,m^2N^{-1}]$		
s_{11}^{E}	4.930	4.87	4.86	1.11	0.966
s_{12}^{E}	–0.519	–0.58	–0.29	–3.83	–16.9
s_{13}^{E}	–1.280	–1.25	–1.24	2.14	12.8
s_{14}^{E}	0.588	0.64	0.63	7.74	15.0
s_{33}^{E}	4.317	4.36	4.36	1.24	6.72
s_{44}^{E}	10.46	10.8	10.5	0.60	–1.18
s_{66}^{E}	10.90	10.9	10.3	0.64	–0.73
Piezoelectric stress constants	$[Cm^{-2}]$	$[Cm^{-2}]$	$[Cm^{-2}]$		
e_{15}	2.72	2.6	2.7	–1.32	–7.17
e_{22}	1.67	1.6	2.0	–0.60	–6.28
e_{31}	–0.38	0.0	–0.1	0.87	51.8
e_{33}	1.09	1.9	2.0	1.54	1.41
Piezoelectric strain constants	$[\cdot 10^{-11}\,CN^{-1}]$	$[\cdot 10^{-11}\,CN^{-1}]$	$[\cdot 10^{-11}\,CN^{-1}]$		
d_{15}	2.64	2.6	2.6	–1.31	–9.64
d_{22}	0.75	0.7	0.85	–1.32	–9.79
d_{31}	–0.30	–0.2	–0.30	+3.27	43.1
d_{33}	0.57	0.8	0.92	+2.74	118.0
Dielectric constants					
κ_{11}^{S}	42.6	41	41	3.29	4.28
κ_{33}^{S}	42.8	43	42	11.6	78.0
κ_{11}^{T}	53.6	51	53	2.11	0.100
κ_{33}^{T}	43.4	45	44	11.47	80.8

Table 2A-2-005. $LiTaO_3$. Values of dielectric constant at 293 K. Parameter: *f*. [a])[88Tom], [b])[75Tea], [c])[70Bar], [d])[67Kam].

	Capacitance measurements [a])					[b])
f	10 kHz	100 kHz	1 MHz	10 MHz	13 MHz	1 GHz
κ_{11}	53.5	53.5		41.7	40.6	40.3
κ_{33}	42.4	42.2	42.0	39.2	38.8	41.4
	Infrared reflectivity [c])				Raman scattering [d])	
κ_{11}^{S}	41.5				41	
κ_{33}^{S}	37.6				43	

Table 2A-2-006. $LiTaO_3$. $c_{\lambda\mu}$, $e_{i\lambda}$. $c_{\lambda\mu}$: elastic stiffness; $e_{i\lambda}$: piezoelectric stress constant.

Ref.	94Tak	91Mur	67War1
c_{11} [$\cdot 10^{11}$ Nm^{-2}]	2.332	2.178	2.33
c_{13}	0.837	0.643	0.80
c_{14}	−0.106	−0.114	−0.11
c_{33}	2.781	2.494	2.75
c_{44}	0.948	0.963	0.94
c_{66}	0.935	0.950	0.93
e_{15} [Cm^{-2}]	2.56	(2.6)	2.6
e_{22}	1.74	(1.6)	1.6
e_{33}	1.80	(1.9)	1.9
e_{31}	−0.21	(0.0)	0.0

Table 2A-2-007. $LiTaO_3$. Summary of design data for microwave surface acoustic wave devices [73Sza]. prop: propagation, Vac attn: (surface wave) attenuation in vacuum, Sw: surface wave, bw: bandwidth.

Orientation	*Z* cut *Y* prop	*Y* cut *Z* prop	22° rotated cut *X* prop	Orientation	*Z* cut *Y* prop	*Y* cut *Z* prop	22° rotated cut *X* prop
Surface wave velocity v_∞ [m s^{-1}]	3329	3230	3302	3 dB Air prop loss time delay at 1 GHz, *A* [μs]	3.0	2.6	
Estimate of electromagnetic to acoustic coupling $\Delta v/v_\infty$	0.0059	0.0033	0.0027	Slope of electromechanical power flow curve $\partial\phi/\partial\theta$ [b])	–1.241	–0.211	+0.764
Measured value of $\Delta v/v_\infty$ [a])	0.0045	0.0036		Slope of electromechanical power flow curve $\partial\phi/\partial\mu$ [c])	+0.556	–0.229	0
Power flow angle ϕ [°] (electromechanical)	0	0	0	3 dB Beam steering loss time delay *B* [μs]	4.4	15.6	13.3
Temperature coefficient of delay $\frac{1}{\tau}\frac{\partial\tau}{\partial T}$ [$\cdot 10^{-6}K^{-1}$]	69.0	35.0	68.0	3 dB Diffraction loss time delay at 1 GHz, *C* [μs]	11.3	3.6	1.6
Sw attn in air at 1 GHz [dB/μs]	1.0	1.14		Material figure of merit F_M $F_M = ABC\left(\frac{\Delta v}{v_\infty}\right)^2$	0.005	0.002	
Air loading at 1 GHz [dB/μs]	0.23	0.20		Time-bw product Figure of merit F_{TB}	0.006	0.002	
Vac attn at 1 GHz [dB/μs]	0.77	0.94		$F_{TB} = \frac{4\cdot 10^3 ABC}{v_\infty}\cdot\left(\frac{\Delta v}{v_\infty}\right)^2$			

[a]) [72Sch2]. [b]) θ: direction of propagation. [c]) μ: direction of plate normal.

Table 2A-2-008. $LiTaO_3$. Surface acoustic wave properties of *X*-cut 112° rotated *Y* propagation mode [82Yas2]. TCD: temperature coefficient of propagation delay time. IDT: interdigital transducer.

v_s	k_s^2	Coupling per unit length of IDT	TCD
3295 ms^{-1}	$8 \cdot 10^{-3}$	6.5 pF/cm pair	$-18 \cdot 10^{-6} K^{-1}$

Table 2A-2-009. $LiTaO_3$. Refractive indices [65Bon].

λ [μm]	n_o	n_e	λ [μm]	n_o	n_e
0.45	2.2420	2.2468	2.00	2.1066	2.1115
0.50	2.2160	2.2205	2.20	2.1009	2.1053
0.60	2.1834	2.1878	2.40	2.0951	2.0993
0.70	2.1652	2.1696	2.60	2.0891	2.0936
0.80	2.1538	2.1578	2.80	2.0825	2.0871
0.90	2.1454	2.1493	3.00	2.0755	2.0299
1.00	2.1391	2.1432	3.20	2.0680	2.0727
1.20	2.1305	2.1341	3.40	2.0601	2.0649
1.40	2.1236	2.1273	3.60	2.0513	2.0561
1.60	2.1174	2.1213	3.80	2.0424	2.0473
1.80	2.1120	2.1170	4.00	2.0335	2.0377

Table 2A-2-010. $LiTaO_3$. Electrooptic constants.

	r_{13}	r_{33}	r_{51}	r_{22}	r_c	λ	Ref.
	$[\cdot 10^{-12}$ m $V^{-1}]$					[μm]	
r^T					22	0.633	66Len
	8.4	30.5				0.633	72Onu
r^S	7	30.3	20	≈1		0.633	66Len
	4.5	27	15	≈0.3		3.39	66Tur

Table 2A-2-011. $LiTaO_3$. Piezooptic constants for λ = 633 nm.

	[76Ava]	[67Dix]		[76Ava]	[67Dix]
p_{11}	–0.081(3)	0.0804	p_{33}	–0.044(4)	0.150
p_{12}	0.081(3)	0.0804	p_{41}	–0.085(6)	0.024
p_{13}	0.093(2)	0.094	p_{44}	0.028(2)	0.022
p_{14}	–0.026(2)	0.031	p_{66}	–0.081(4)	
p_{31}	0.089(4)	0.086			

Table 2A-2-012. $LiTaO_3$. Pressure derivatives of refractive indices [81Cor].

λ [nm]	dn_o/dp [$\cdot 10^{-2}$ GPa^{-1}]	dn_e/dp [$\cdot 10^{-2}$ GPa^{-1}]
509.0	0.088	0.209
546.1	0.099	0.221
598.3	0.109	0.227

Table 2A-2-013. $LiTaO_3$. Assignment of Raman active modes (wave number shifts in cm^{-1}) in the ferroelectric phase (290 K). The superscripts ⊥, ‖ and / indicate directions of phonon propagation perpendicular, parallel, and at 45° relative to the unique axis.

A_1 Modes:

[67Kam]		[76Pen1]		[87Yan]		[88Rap]	
TO	LO	TO	LO	TO	LO	TO	LO
201	245	81	82	206	252	$203^{\perp}$	$250^{\parallel}$
253	347	186	200	253	354	$252^{\perp}$	$287^{\parallel}$
356	399	202	246	356	402	$356^{\perp}$	$438^{\parallel}$
600	864	250	354	600	865	$597^{\perp}$	$864^{\parallel}$
		355	401				
		458	465				
		594	660				
		661	750				
		751	866				

E Modes:

[67Kam]		[76Pen1]		[87Yan]		[88Rap]	
TO	LO	TO	LO	TO	LO	TO	LO
74	80	69	70	142	142	$142^{\perp,/}$	$142^{\perp}$
140	163	141	200	142	190	$(142^{\perp}?)$	$194^{\perp}$
206	248	249	275	206	206	$207^{\perp,/}$	$278^{\perp}$
251	278	316	345	252	280	$(314^{\perp}?)$	$314^{\perp}$
316	318	345	379	315	315	$314^{\perp,/}$	$344^{\perp}$
383	452	382	459	315	380	$355^{\perp,/}$	$378^{\perp}$
462	474	462	470	382	463	$382^{\perp,/}$	$445^{\perp}$
596	648	591	659	463	463	$463^{\perp,/}$	$463^{\perp}$
662	870	660	866	592	866	$592^{\perp,/}$	$865^{\perp}$

Table 2A-2-014. $LiTaO_3$. Brillouin scattering [71Kha]. Geometry [for example $z(xz)y$] from left to right: propagation direction of the incident light, polarization of the incident light, polarization of the scattered light and propagation direction of the scattered light. Direction: phonon propagation direction, $\Delta\nu$: phonon frequency, *: intense lines, υ_{exp}: experimental phonon velocity, P: phonon polarization, ql: quasi-longitudinal, qt: quasi-transverse, t: transverse.

Geometry	Direction	$\Delta\nu/c$ [$\cdot 10^2$ m^{-1}]	υ_{exp} [$\cdot 10^3$ m s^{-1}]	P
$x(zx)\bar{y}$	$k_x=-\frac{\sqrt{2}}{2}$; $k_y=-\frac{\sqrt{2}}{2}$	1.15	6.89	ql
		0.72	4.32	qt
$x(zz)\bar{y}$	$k_z=0$	1.10	6.71	ql
$y(zy)x$	$k_x=\frac{\sqrt{2}}{2}$; $k_y=-\frac{\sqrt{2}}{2}$	0.66*	3.96	qt
$y(zz)x$	$k_z=0$	1.10	6.71	ql
$z(xz)y$	$k_x=0$; $k_y=\frac{\sqrt{2}}{2}$	0.58*	3.48	t
$z(xx)y$	$k_z=-\frac{\sqrt{2}}{2}$	1.21	7.11	ql
$x(xz)\bar{y}$	$k_x=0$	0.59*	3.54	t
$x(xx)\bar{y}$	$k_y=-\frac{\sqrt{2}}{2}$	1.23	7.23	ql
$x(yz)\bar{y}$		0.59	3.54	qt
$x(yx)\bar{y}$	$k_z=-\frac{\sqrt{2}}{2}$	0.61	3.58	qt
$z(yz)x$	$k_x=-\frac{\sqrt{2}}{2}$; $k_y=0$	0.62*	3.72	qt
$z(yy)x$	$k_z=-\frac{\sqrt{2}}{2}$	0.64	3.76	qt
		1.22	7.17	ql

Table 2A-2-015. $LiTaO_3$. ESR data.

Paramagnetic center	Cr^{3+}	Mn^{2+}
H	(4)	(8)
ν [GHz]		X and K band
T		RT
g-factor	$g_{\parallel} = 1.971$ $g_{\perp} = 3.863$	$g_{\parallel} = g_{\perp} = 1.995(5)$
FS $[\cdot 10^{-2}\,m^{-1}]$	$D = 4300(500)$	$b_{20} = 1694(14)$ $b_{40} = -12(16)$
HFS $[\cdot 10^{-2}\,m^{-1}]$		$A_{\parallel} = -78.2(5)$ $A_{\perp} = -76.4(5)$
Ref.	68Bur	68Dan

Table 2A-2-016. $LiTaO_3$. Spin Hamiltonian parameters for Cu^{2+} center [85Kha]. T = 77 K.

Principal values of g-tensor	Principal values of A-tensor [$\cdot 10^{-2}$ m^{-1}]
$g_z = 2.396(4)$	$A_z = 70(1)$
$g_y = 2.099(5)$	$A_y = 50(2)$
$g_x = 2.050(4)$	$A_x = 56(1)$
$g'_{\parallel} = 2.19(1)$	
$g'_{\perp} = 2.16(1)$	

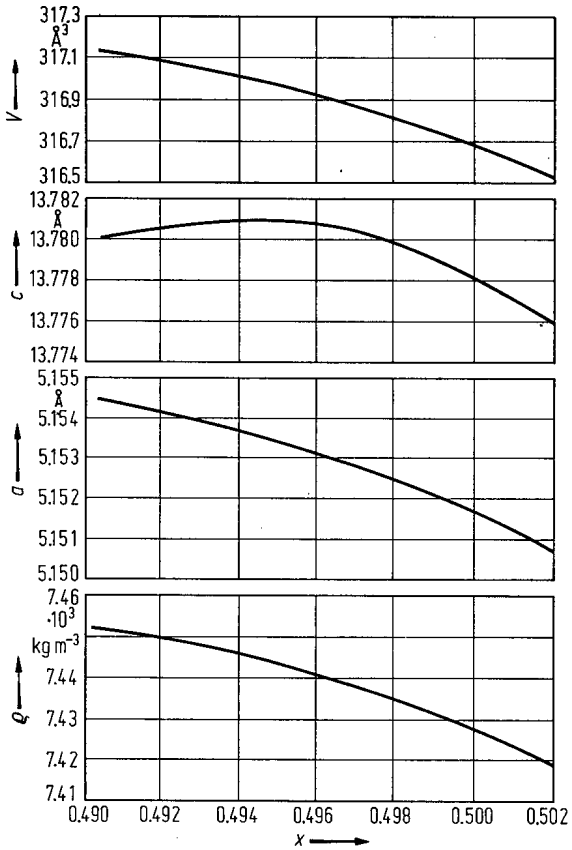

Fig. 2A-2-001. $LiTaO_3$. Lattice parameters and density of crystals grown from x $Li_2O{\cdot}(1–x)Ta_2O_5$ melt vs. x [70Bar1]. *V*: unit cell volume, ρ: density.

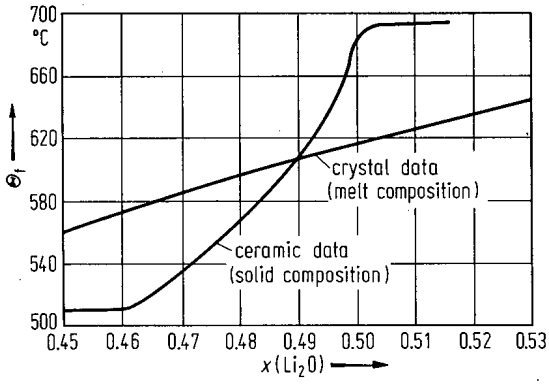

Fig. 2A-2-002. $LiTaO_3$. Θ_f vs. x. Crystal data: Θ_f of crystals grown from x $Li_2O{\cdot}(1–x)Ta_2O_5$ melt [67Bal]. Ceramic data: Θ_f of ceramics sintered from x $Li_2O{\cdot}(1–x)Ta_2O_5$ system [70Bar1]. See also [68Yam1, 71Miy].

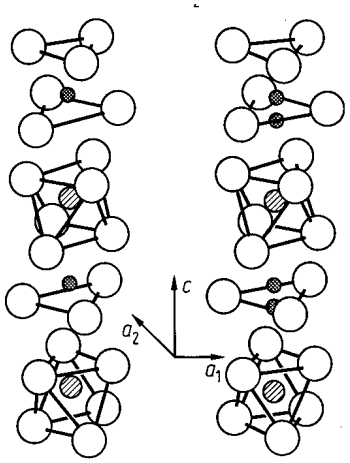

Fig. 2A-2-003. $LiTaO_3$. (**a**) Polar arrangement of oxygen atom (large circle) octahedra in $LiTaO_3$ stacked along the trigonal axis. The octahedra contain, in sequence, a Ta atom (hatched circles), no metal atom, and Li atom (cross-hatched circles). (**b**) Arrangement of atoms above the ferroelectric transition temperature within one stack of octahedra. The Ta atom is at an octahedron center and the Li atom is distributed within the next two octahedra [73Abr].

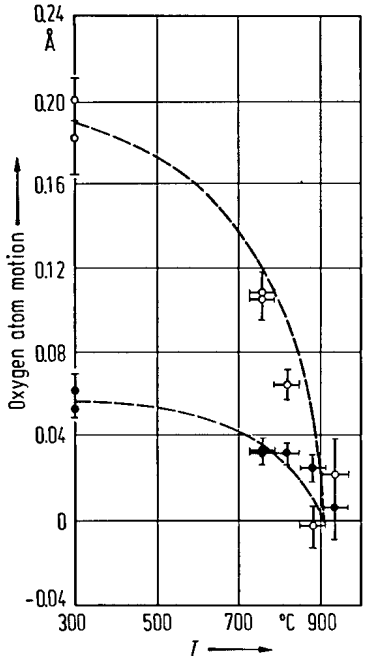

Fig. 2A-2-004. $LiTaO_3$. Variation of oxygen shifts vs. *T* [73Abr]. Full circles: *y* (O)–1/3, open circles: 1/12–*z*(O). The dashed lines are the variation of P_s with *T*, normalized to the diffraction data at 298 °C and 907 °C.

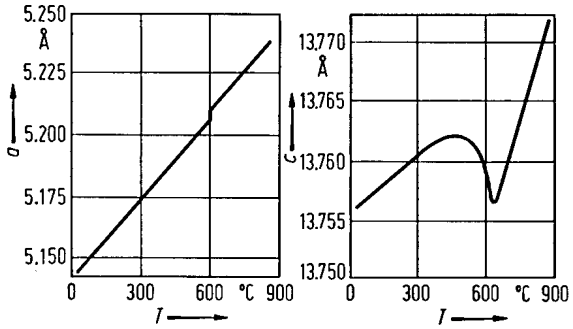

Fig. 2A-2-005. $LiTaO_3$. *a*, *c* vs. *T* [67Iwa]. Thermal expansion was measured by the dilatometric method.

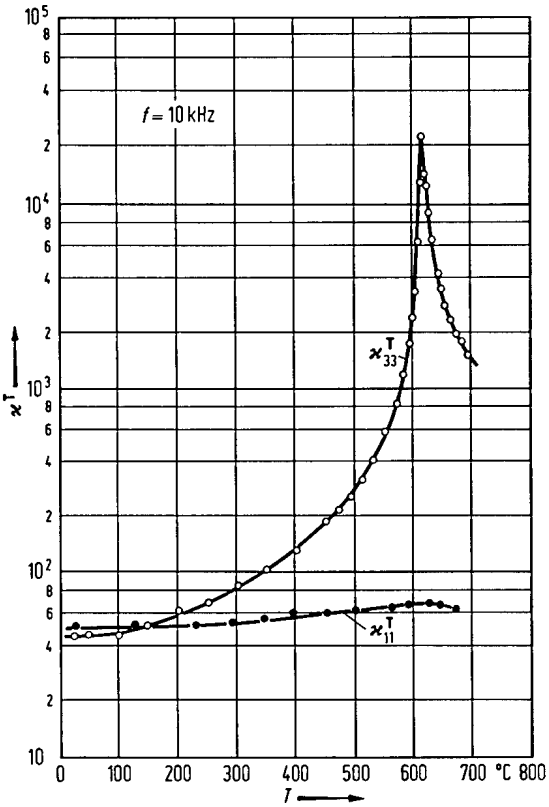

Fig. 2A-2-006. $LiTaO_3$. κ_{33}^T, κ_{11}^T vs. T [68Yam2]. f = 10 kHz.

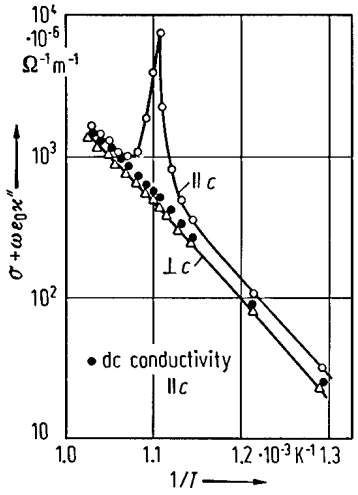

Fig. 2A-2-007. $LiTaO_3$. $\sigma + \omega\varepsilon_0\kappa''$ vs. T^{-1} [69Yam]. Open circles and triangles: f = 10 kHz. Full circles: f = 0 Hz.

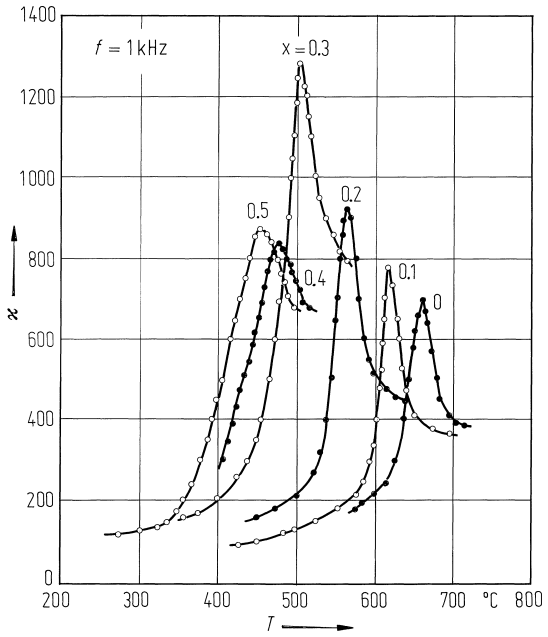

Fig. 2A-2-008. $Li_{1-x}Zn_{x/2}TaO_3$ (ceramics). κ vs. T [83Tor]. Parameter: x. f = 1 kHz.

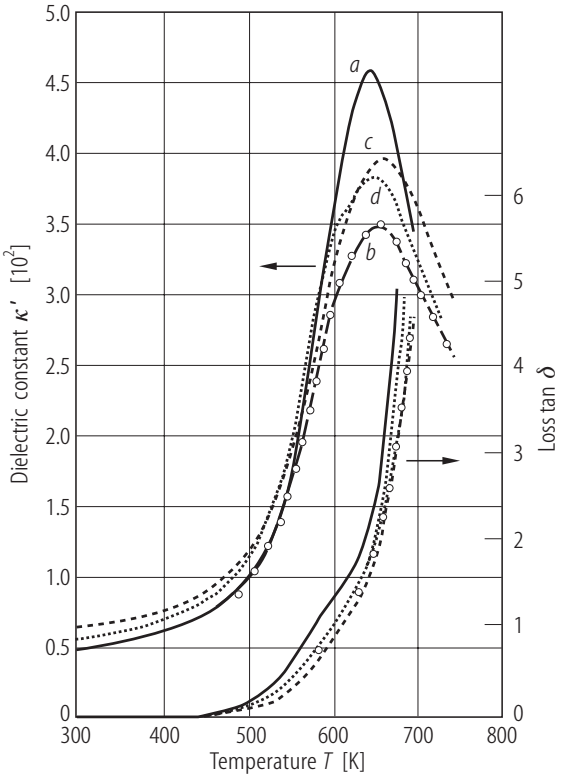

Fig. 2A-2-009. $LiTaO_3$ (ceramics). κ', $\tan\delta$ vs. T [90InH]. Sintering time: *a*: 4 h, *b*: 2 h, *c*: 0.5 h, *d*: 0.25 h. f = 1 kHz.

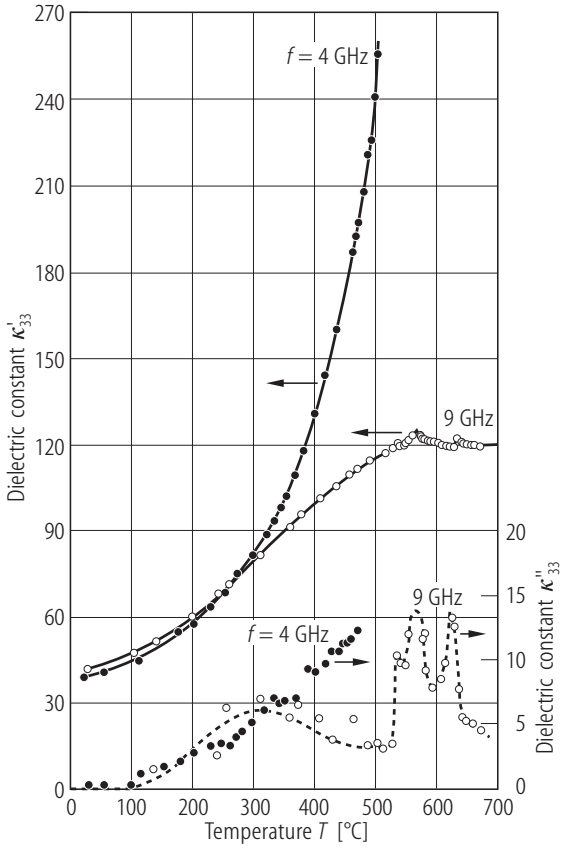

Fig. 2A-2-010. $LiTaO_3$. κ'_{33}, κ''_{33} vs. T [70Saw]. Parameter: f.

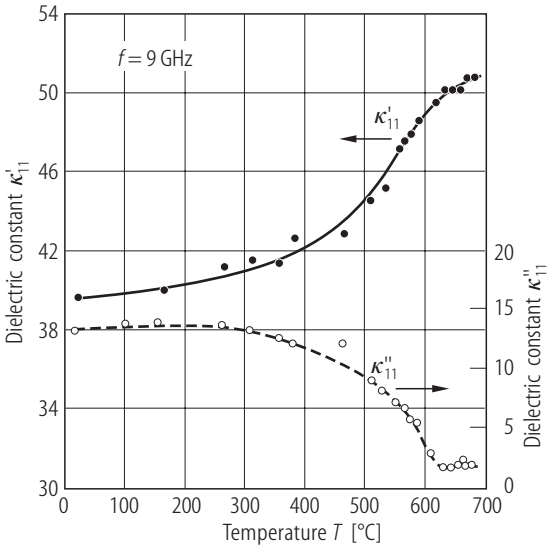

Fig. 2A-2-011. $LiTaO_3$. κ'_{11}, κ''_{11} vs. T [70Saw]. f = 9 GHz.

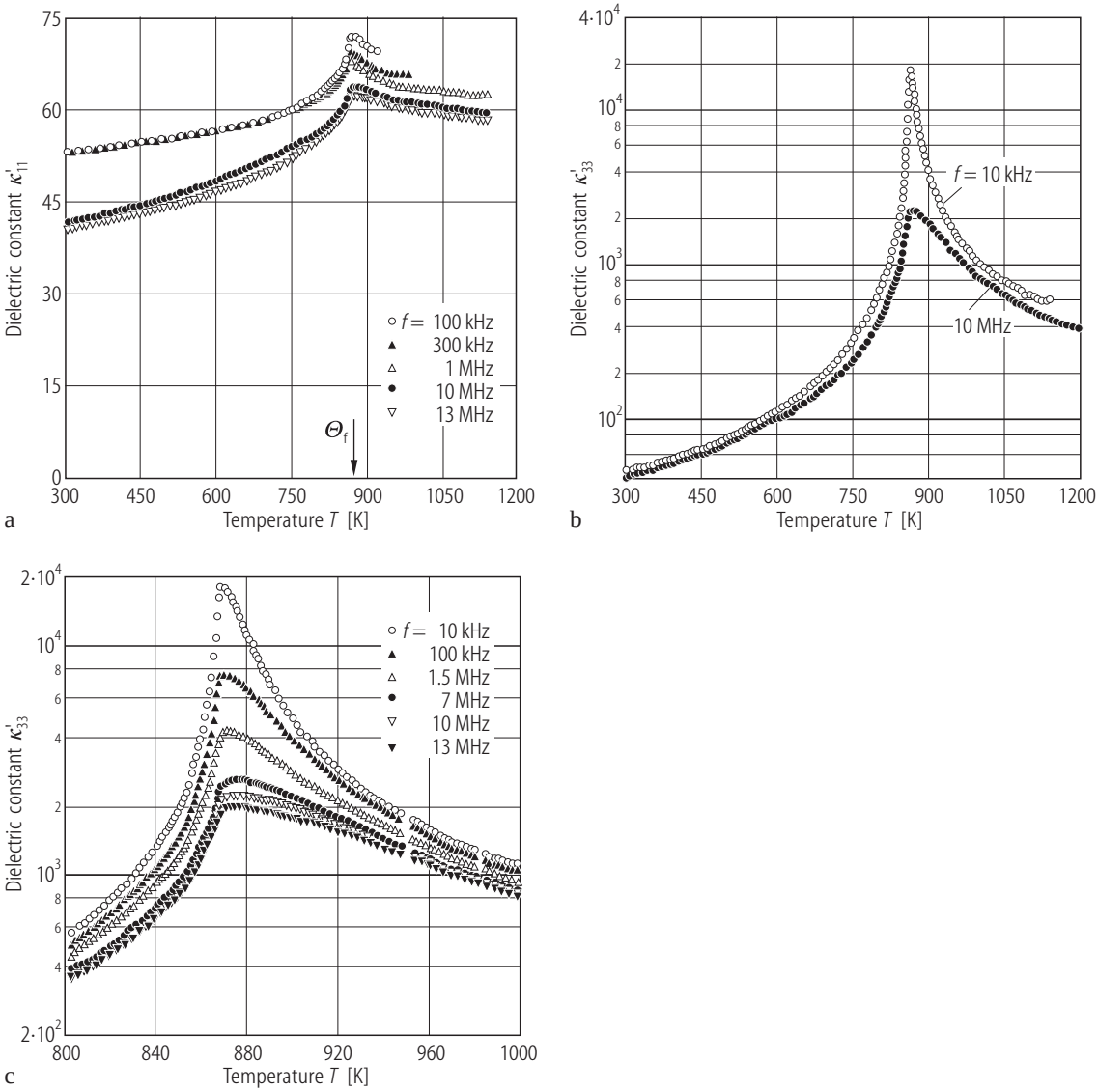

Fig. 2A-2-012. $LiTaO_3$. κ'_{ii} vs. T [88Tom]. Parameter: f.

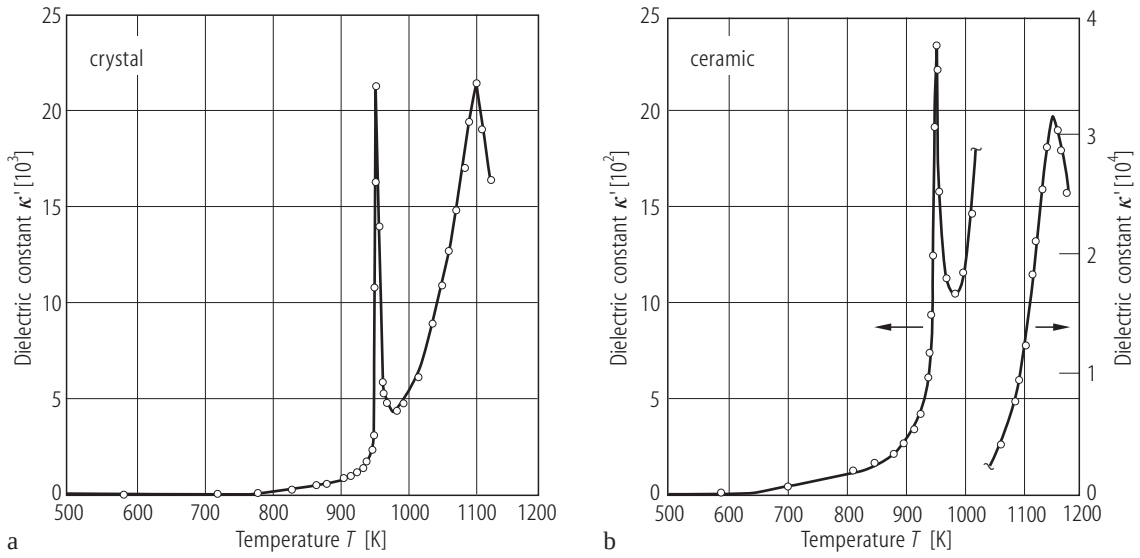

Fig. 2A-2-013. $LiTaO_3$. κ' vs. T [90YeZ]. f = 1 kHz. (**a**) single crystal. (**b**) ceramics.

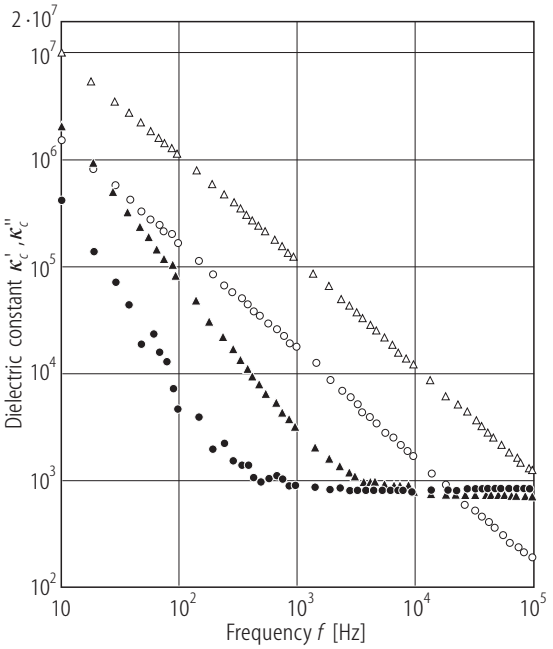

Fig. 2A-2-014. $LiTaO_3$. κ'_c, κ''_c vs. f [93Tou]. Triangles: proton-exchanged specimen with exchanged layer of about 3 μm thick. Circles: unprocessed specimen. Full triangles, full circles: κ'_c. Open triangles, open circles: κ''_c.

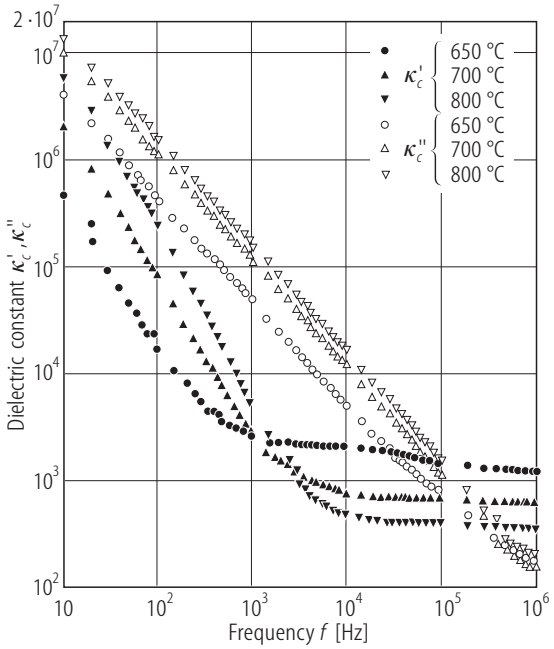

Fig. 2A-2-015. $LiTaO_3$. κ_c' , κ_c'' vs. T of proton-exchanged specimens [93Tou]. Parameter: T. Proton-exchanged layer was estimated to be about 3 μm thick.

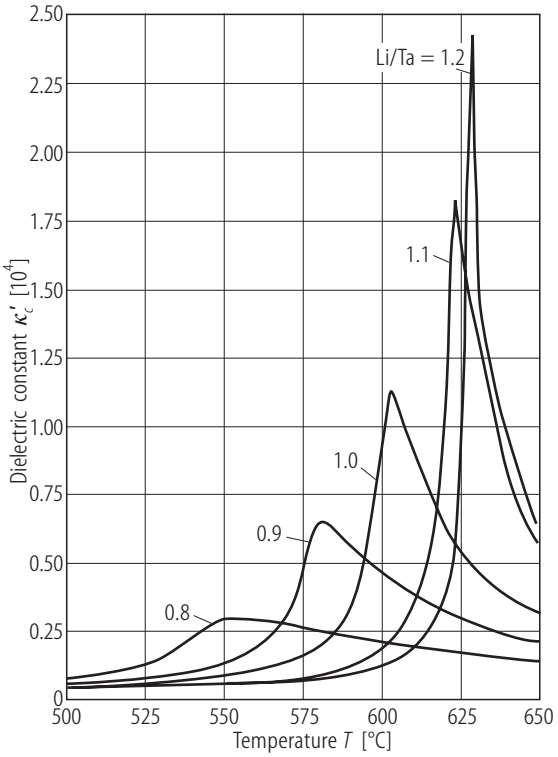

Fig. 2A-2-016. $LiTaO_3$. κ_c' vs. T in various compositions [71Fuj]. f = 1 MHz. Parameter: Li / Ta ratio.

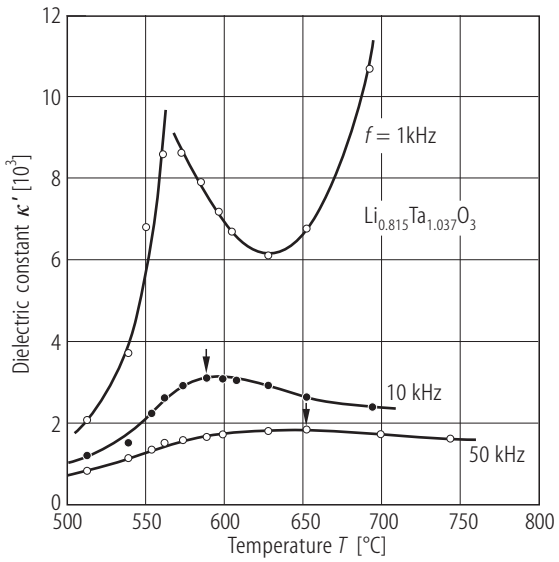

Fig. 2A-2-017. $LiTaO_3$ (nonstoichiometric ceramic). κ' vs. T [87Hua]. Parameter: f. Arrows indicate maximum κ' points.

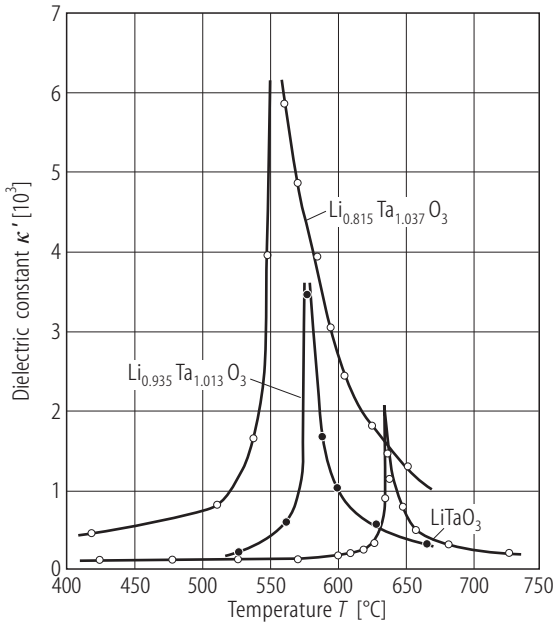

Fig. 2A-2-018. $LiTaO_3$ (ceramics). κ' vs. T [87Hua]. Parameter: Li/Ta stoichiometry.

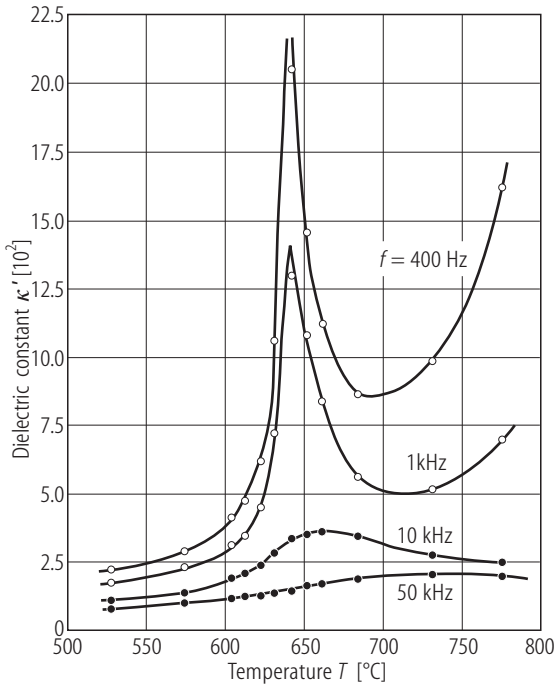

Fig. 2A-2-019. $LiTaO_3$ (stoichiometric ceramic). κ' vs. T [87Hua]. Parameter: f.

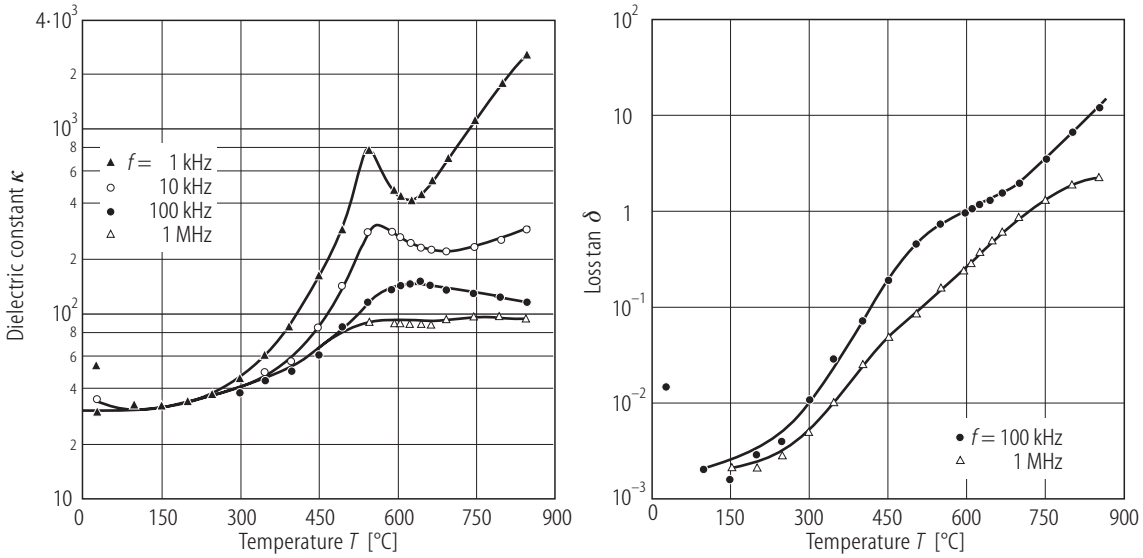

Fig. 2A-2-020. $LiTaO_3$ (ceramic). κ, $\tan\delta$ vs. T [91Chi]. Parameter: f.

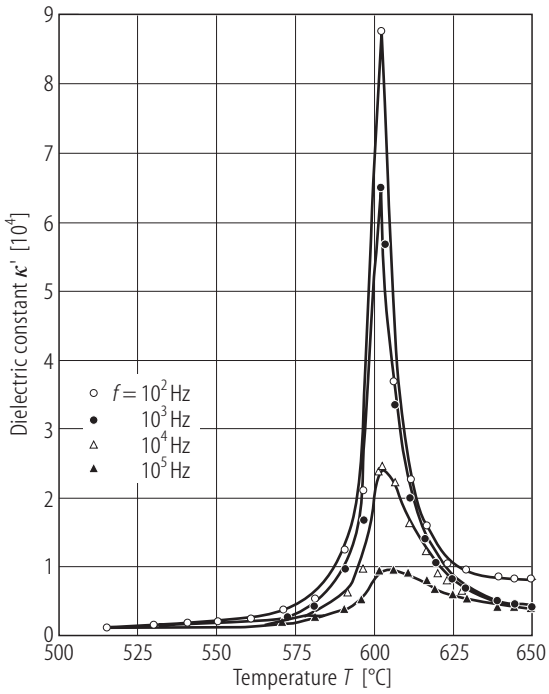

Fig. 2A-2-021. $LiTaO_3$. κ' vs. T [94Rav]. Parameter: f.

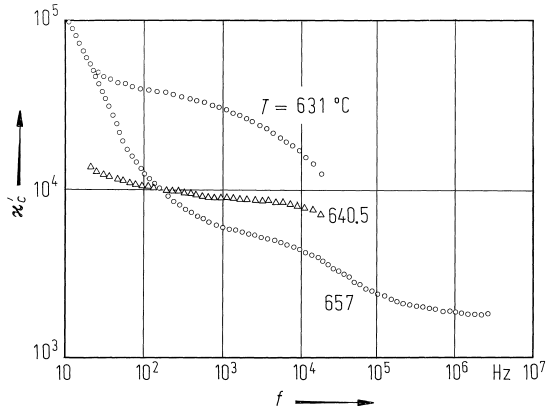

Fig. 2A-2-022. $LiTaO_3$. . κ'_c vs. f [87Pri]. Parameter: T.

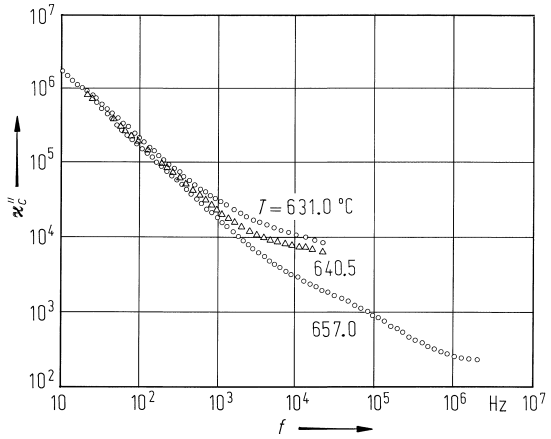

Fig. 2A-2-023. $LiTaO_3$. κ_c'' vs. f [87Pri]. Parameter: T.

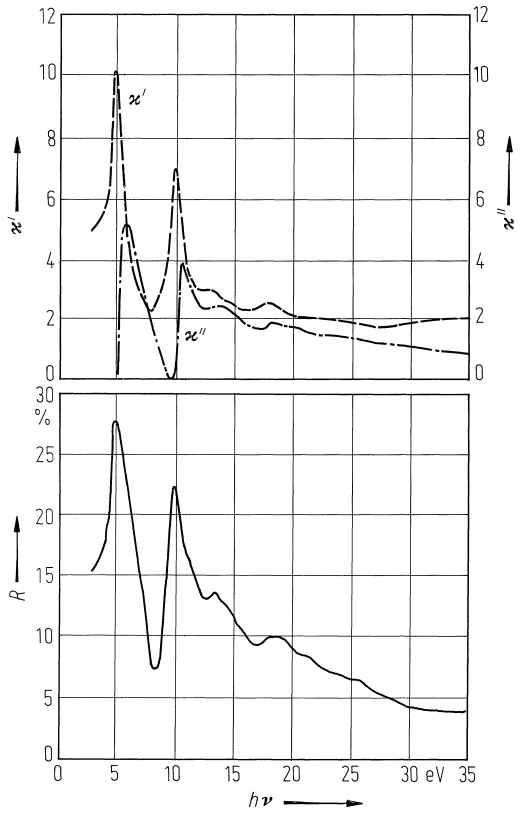

Fig. 2A-2-024. $LiTaO_3$. R, κ', κ'' vs. $h\nu$ at 300 K [83Mam].
$h\nu$: photon energy.

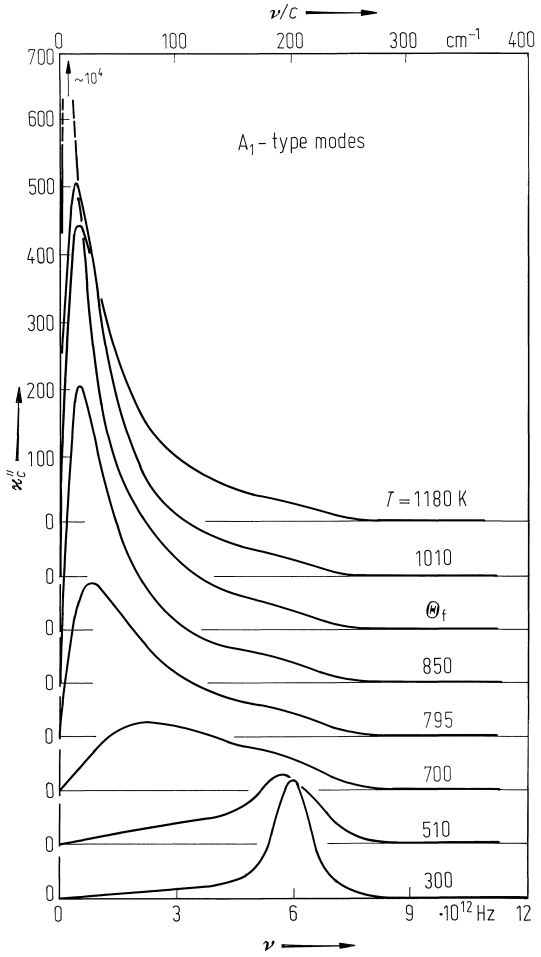

Fig. 2A-2-025. $LiTaO_3$. κ_c'' vs. ν [80Ser]. Parameter: T.

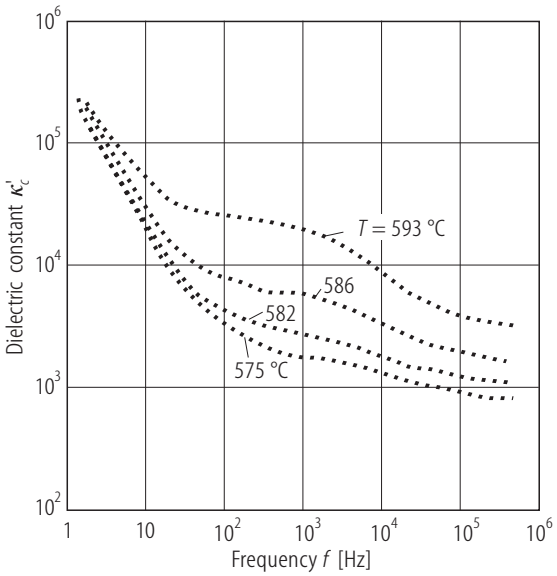

Fig. 2A-2-026. $LiTaO_3$. κ_c' vs. f [89Sin]. Parameter: T.

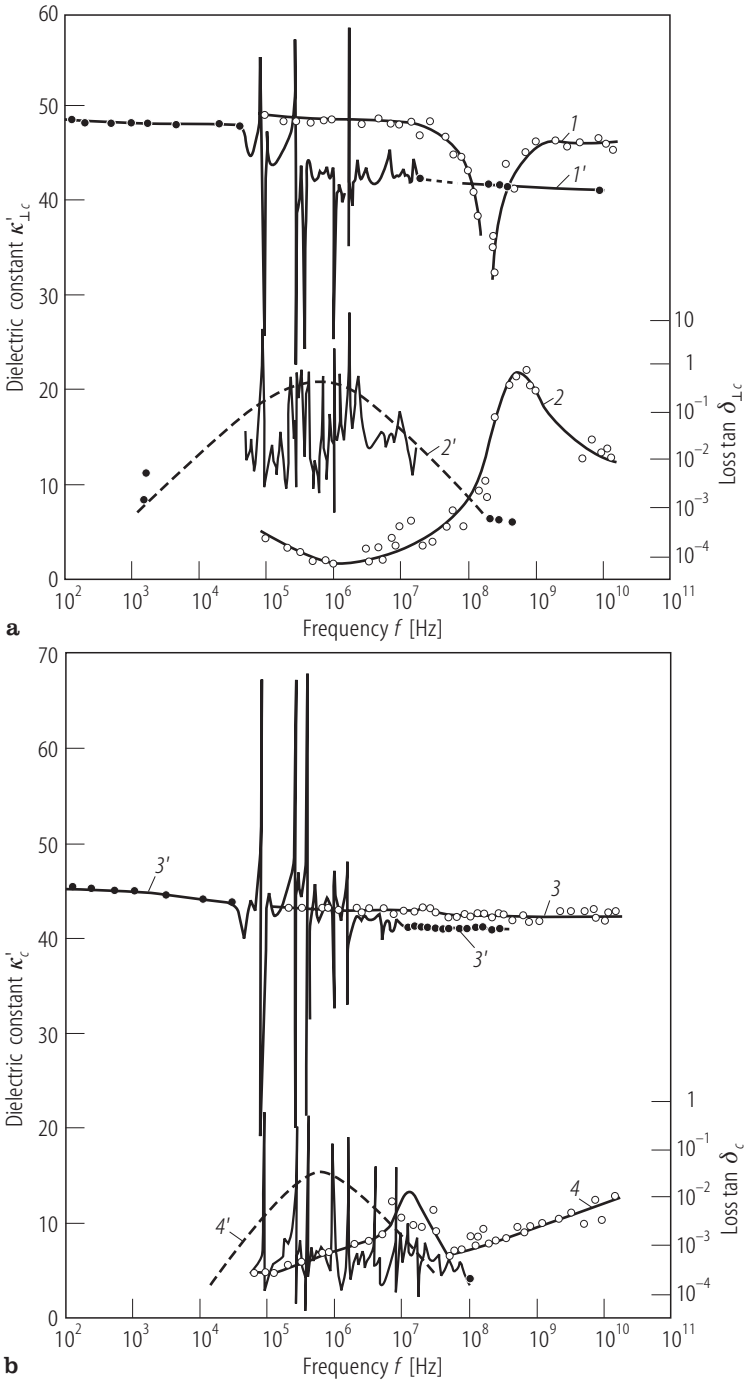

Fig. 2A-2-027. $LiTaO_3$. κ'_c , $\kappa'_{\perp c}$, $\tan\delta_c$, $\tan\delta_{\perp c}$ vs. f [85Bor]. *1...4*: polydomain crystal. *1'...4'*: single domain crystal.

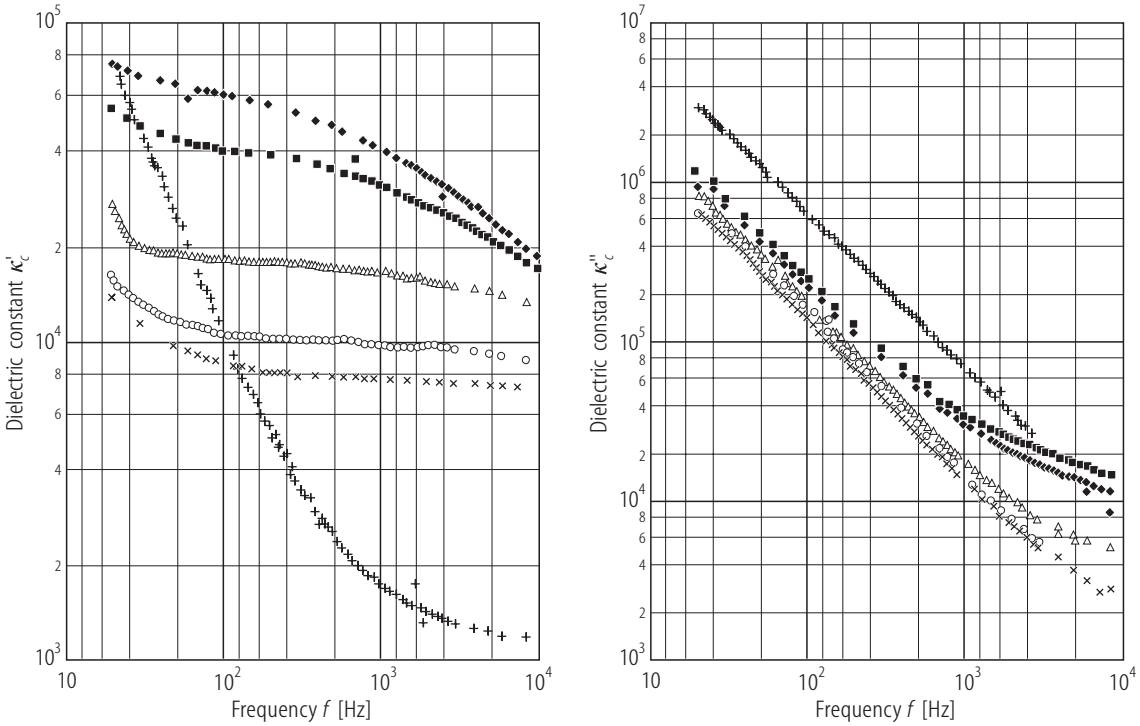

Fig. 2A-2-028. $LiTaO_3$. κ'_c, κ''_c vs. f [86Pri]. Parameter: T. Plus: 755.5 °C, cross: 643 °C, circle: 643.5 °C, triangle: 635.5 °C, square: 631 °C, diamond: 627 °C.

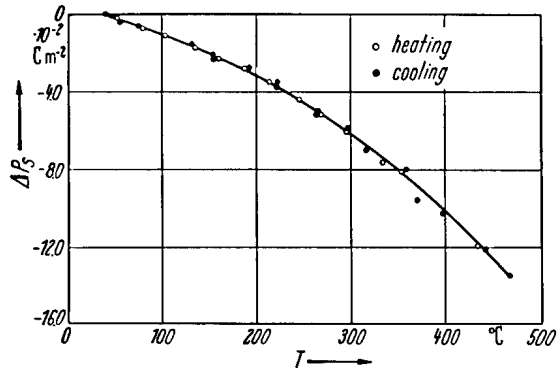

Fig. 2A-2-029. $LiTaO_3$. ΔP_s vs. T [67Iwa]. $\Delta P_s = P_s(0\ °C) - P_s(T)$.

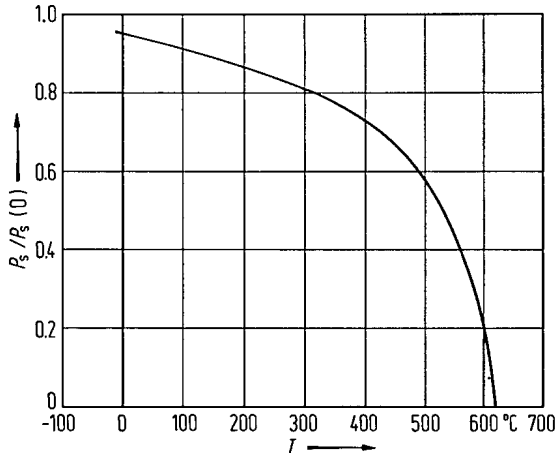

Fig. 2A-2-030. $LiTaO_3$. $P_s/P_s(0)$ vs. T [68Gla]. $P_s(0)$: spontaneous polarization at 0 K.

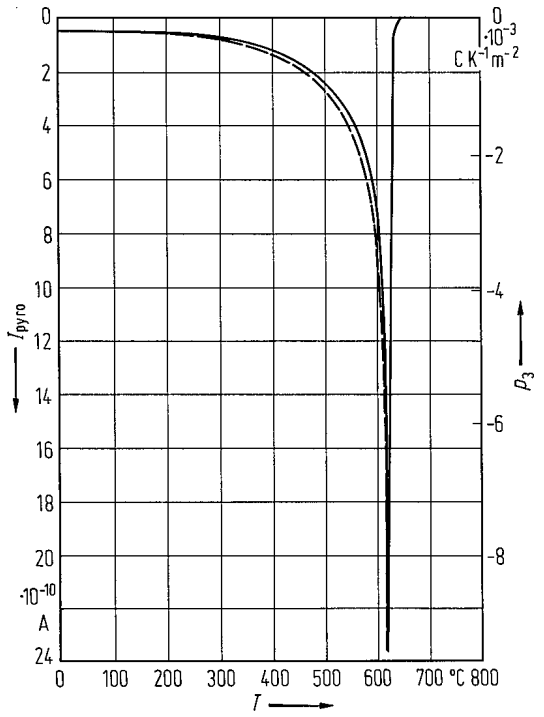

Fig. 2A-2-031. $LiTaO_3$. I_{pyro}, p_3 vs. T [68Gla]. I_{pyro}: pyroelectric current, p_3: pyroelectric coefficient along the c-axis. Dashed curve: corrected for temperature variation of c_p and W, where W is the power absorbed.

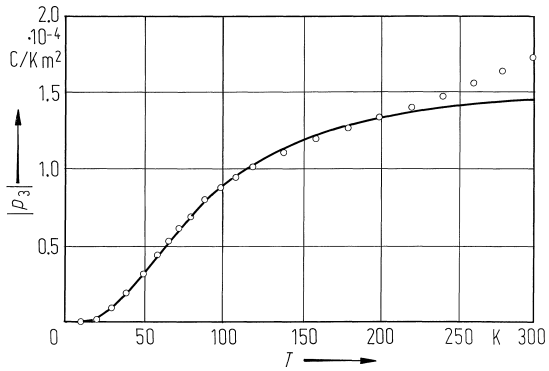

Fig. 2A-2-032. $LiTaO_3$. $|p_3|$ vs. T [77Lin]. Circles: measured values, full curve: sum of two Einstein functions for modes at 81 and 218 cm^{-1}.

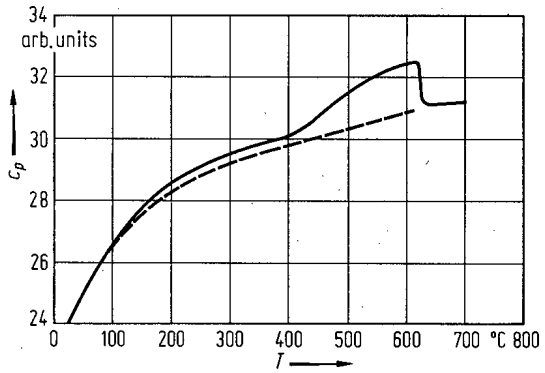

Fig. 2A-2-033. $LiTaO_3$. c_p vs. T [68Gla]. Dashed curve: background specific heat.

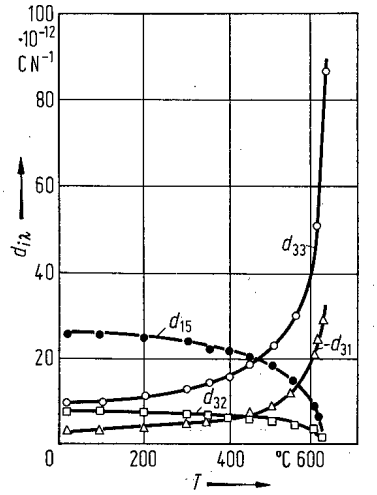

Fig. 2A-2-034. $LiTaO_3$. d_{ik} vs. T [69Yam]. d_{ik}: piezoelectric constant. d_{32} in the figure should be read as d_{22}.

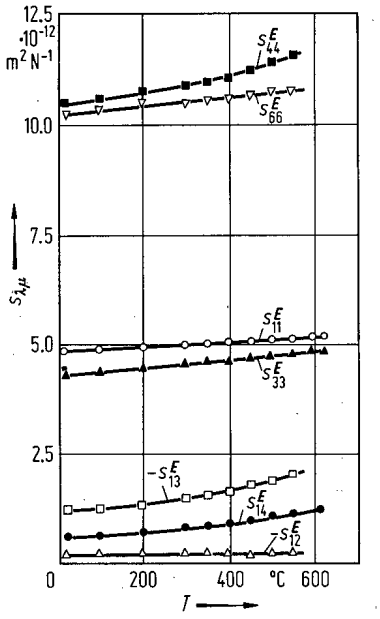

Fig. 2A-2-035. $LiTaO_3$. $s_{\lambda\mu}$ vs. T [69Yam]. $s_{\lambda\mu}$: elastic compliance.

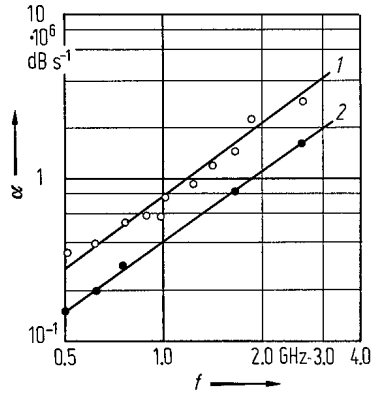

Fig. 2A-2-036. $LiTaO_3$. α vs. f [69Val]. α: attenuation coefficient of ultrasonic wave along the *a*-axis. Curve *1*: transverse wave, *2*: longitudinal wave.

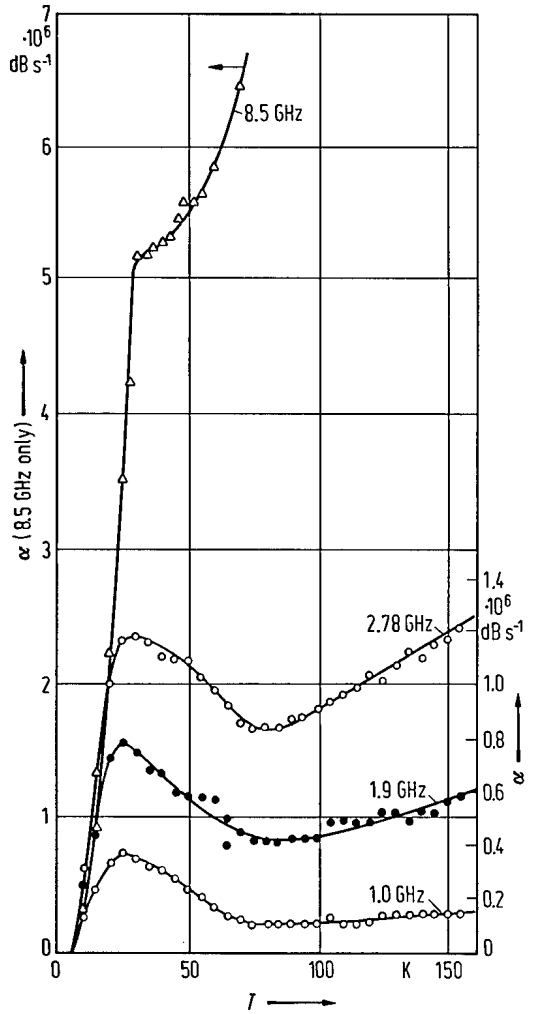

Fig. 2A-2-037. $LiTaO_3$. α vs. T [70Wor]. α: longitudinal wave attenuation in crystal grown from a melt containing 5 mol % excess of Ta_2O_5. Parameter: f.

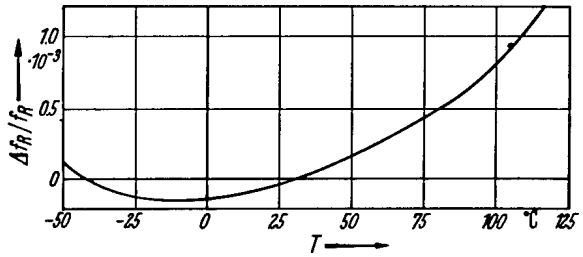

Fig. 2A-2-038. $LiTaO_3$. $\Delta f_R/f_R$ vs. T [67War2]. f_R: resonant frequency of an x-cut plate. Δf_R: frequency variation compared to f_R at 30 °C.

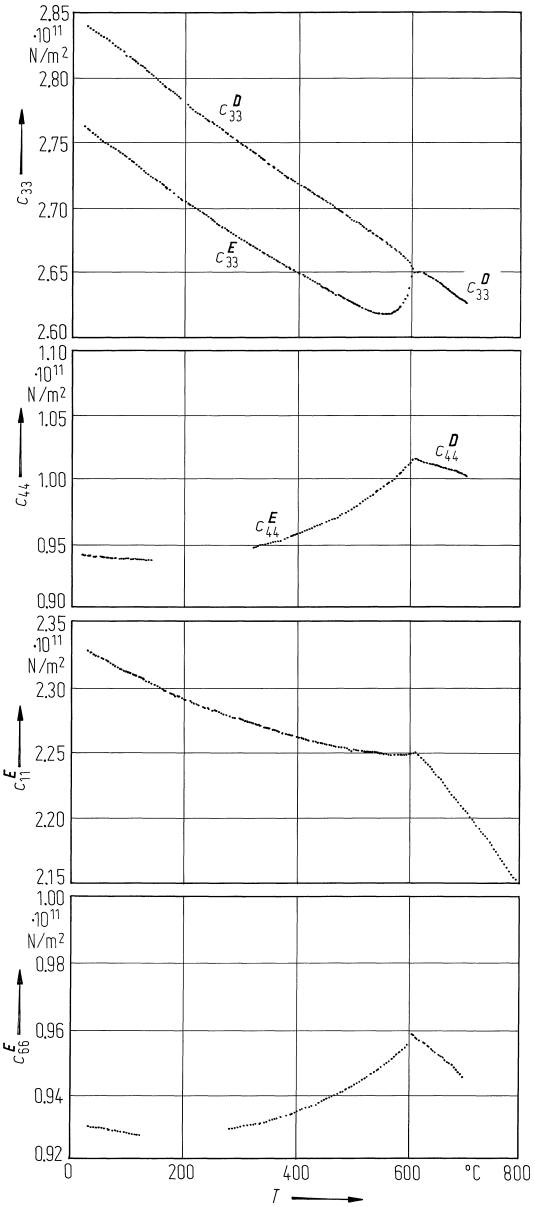

Fig. 2A-2-039. $LiTaO_3$. $c_{\lambda\mu}$ vs. T [82Tom]. $c_{\lambda\mu}$: elastic stiffness. The crystals were grown from approximately congruent melts. Single domain samples. f = 20 MHz.

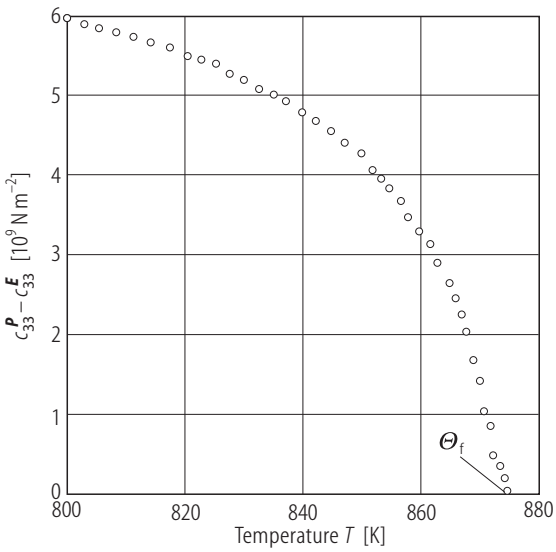

Fig. 2A-2-040. $LiTaO_3$. $c_{33}^{P}-c_{33}^{E}$ vs. T [88Tom].

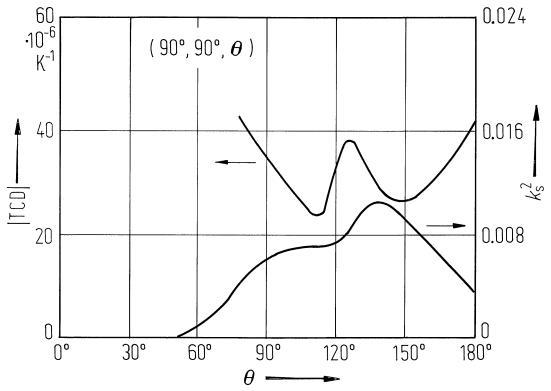

Fig. 2A-2-041. $LiTaO_3$. TCD, k_s^2 vs. θ [85Hir]. TCD: temperature coefficient of surface acoustic wave delay of *X*-cut θ rotated *Y* propagation mode, k_s^2 : surface acoustic coupling constant.

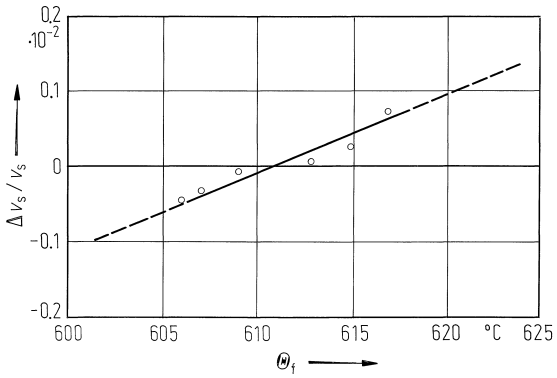

Fig. 2A-2-042. $LiTaO_3$. $\Delta v_s/v_s$ vs. Θ_f [84Yam]. $\Delta v_s/v_s$: normalized surface acoustic wave velocity change of *X*-cut 112° rotated *Y* propagation mode.

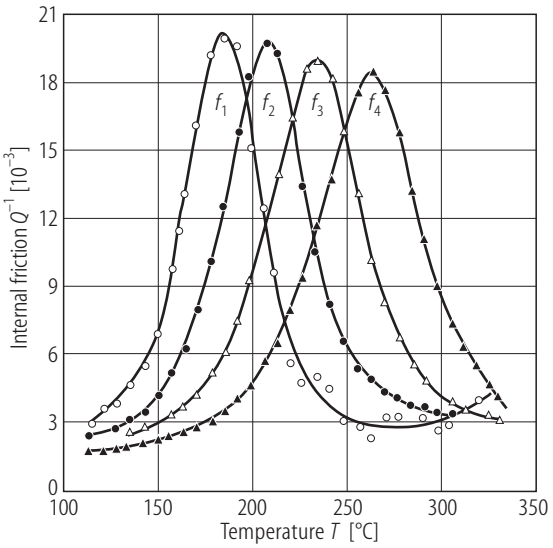

Fig. 2A-2-043. $LiTaO_3$. Q^{-1} vs. T [90Zha]. Q^{-1}: internal friction. Parameter: f. f_1 = 0.0473 Hz, f_2 = 0.224 Hz, f_3 = 1.057 Hz, f_4 = 5.00 Hz.

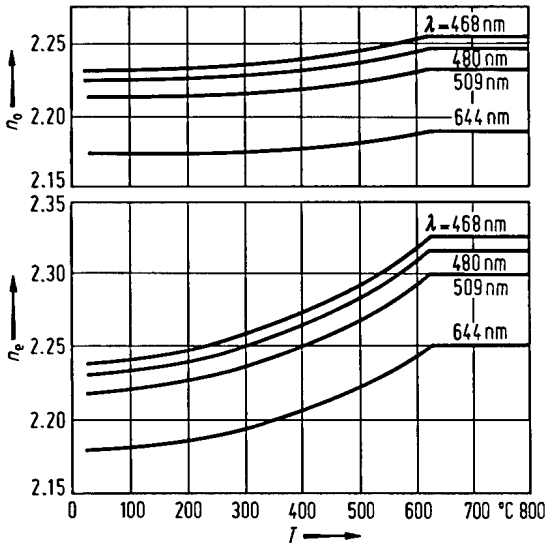

Fig. 2A-2-044. $LiTaO_3$. n_o, n_e vs. T [68Iwa]. Parameter: λ.

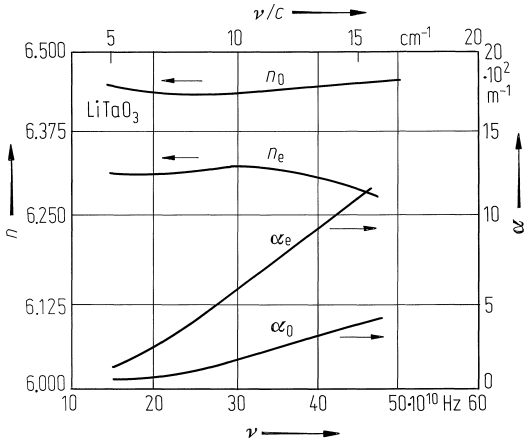

Fig. 2A-2-045. $LiTaO_3$. n, α vs. ν in the near millimeter wave region [83Bro]. α: power absorption coefficient.

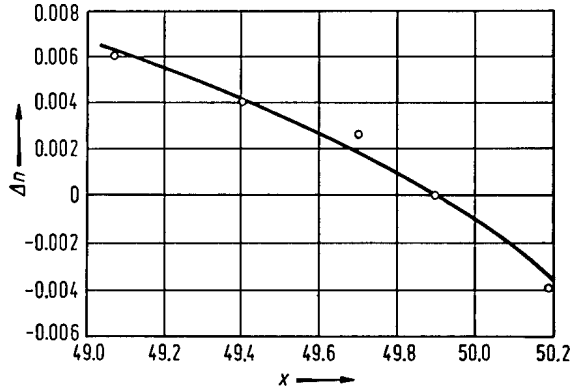

Fig. 2A-2-046. $LiTaO_3$. Δn vs. x [70Bar1]. x: mol % Li_2O in the solid sample determined from Θ_f (see Fig. 2A-2-002). Na-D light was used.

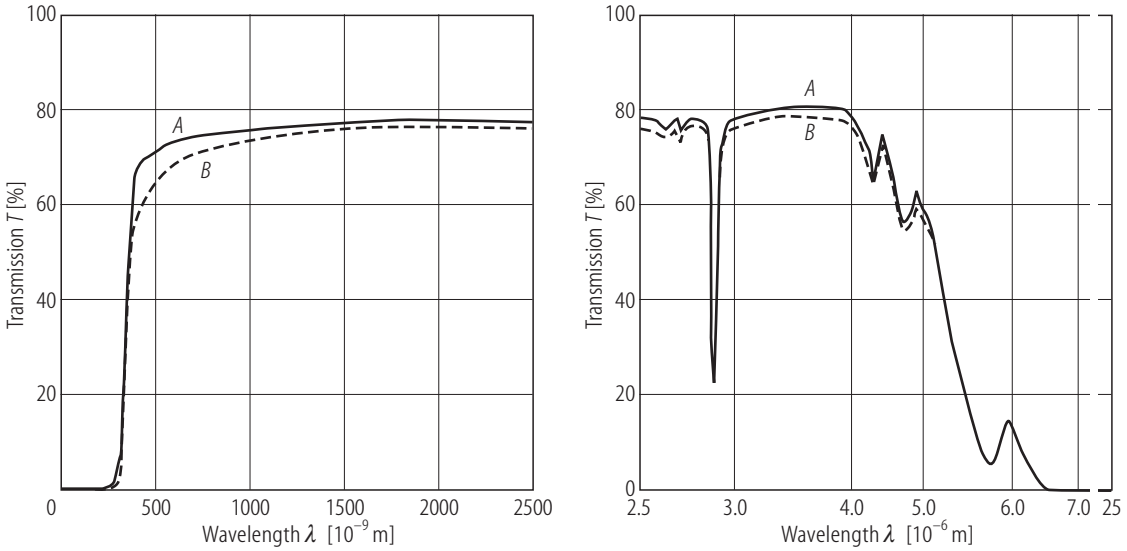

Fig. 2A-2-047. $LiTaO_3$. *T* vs. λ [93Wan]. *T*: light transmission. Sample: *x*-cut $LiTaO_3$ single crystal (d = 3 mm). *A*: poled sample; *B*: annealed sample. Please note changes in horizontal scale.

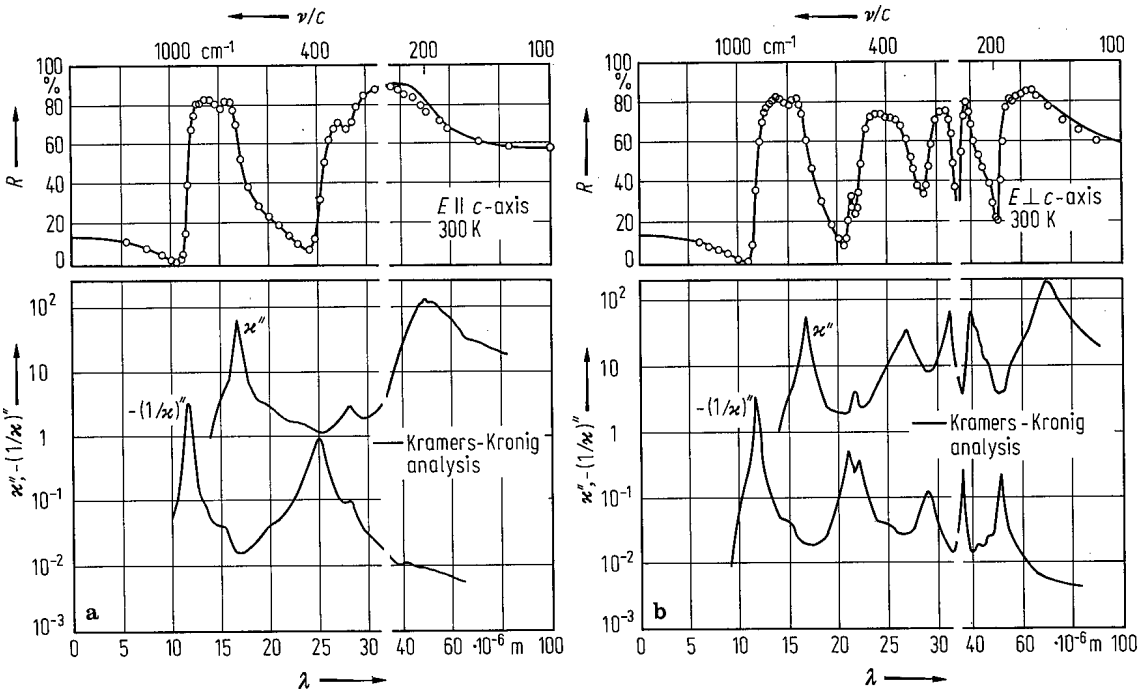

Fig. 2A-2-048. $LiTaO_3$. R, κ'', $-(1/\kappa)''$ vs. λ at 300 K [70Bar2]. R: reflectivity, κ'': imaginary part of κ, $-(1/\kappa)''$: imaginary part of $-1/\kappa$. (**a**) $E \parallel c$, (**b**) $E \perp c$. The solid curves through the experimental points are the best oscillator fit.

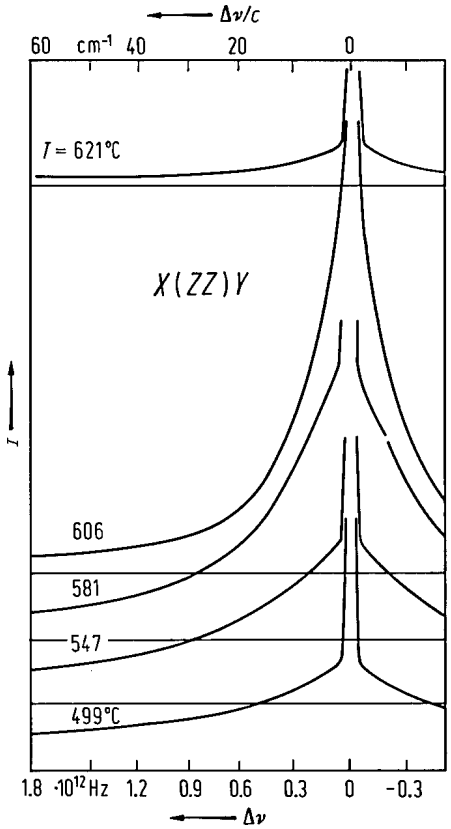

Fig. 2A-2-049. $LiTaO_3$. I vs. $\Delta\nu$ [76Pen2]. I: Raman scattering intensity for the polarization geometry of $X(ZZ)Y$, $\Delta\nu$: frequency shift. For other temperatures, see original paper.

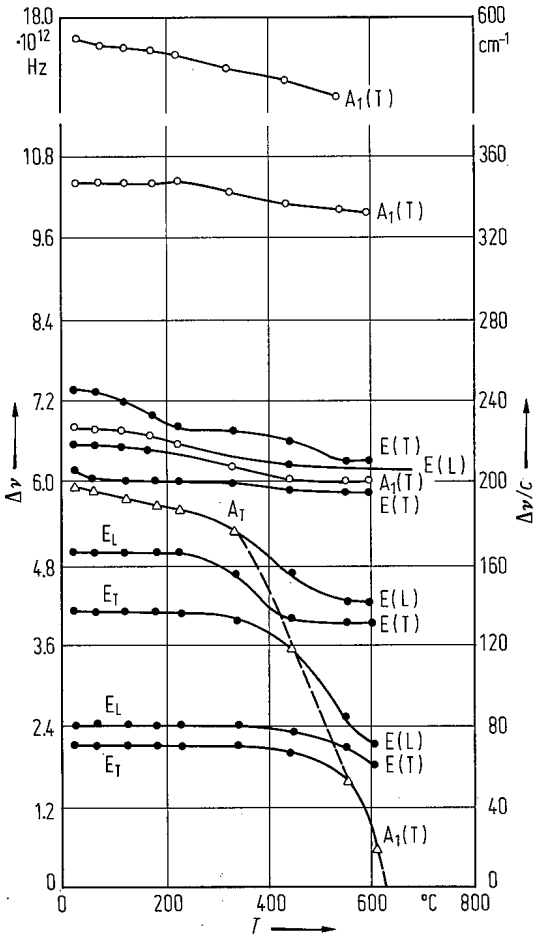

Fig. 2A-2-050. $LiTaO_3$. $\Delta\nu$ vs. T [68Joh]. $\Delta\nu$: Raman frequency shift. Triangles indicate the soft mode peak. Broken lines are mere extrapolation of the data. See also [76Pen1].

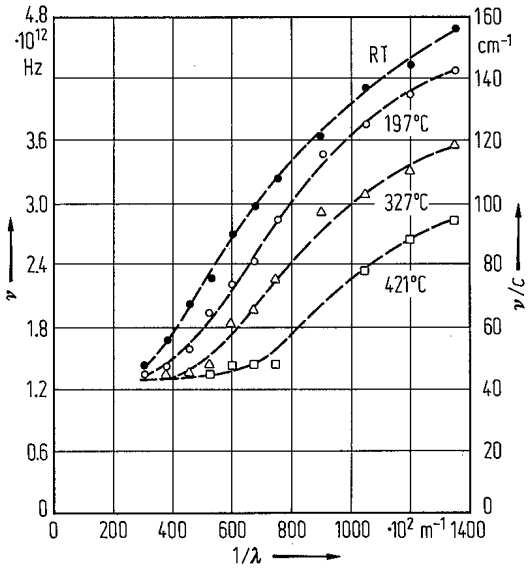

Fig. 2A-2-051. $LiTaO_3$. ν vs. $1/\lambda$ [76Pen3]. ν: polariton frequency of the lowest A_1 phonon mode. Parameter: *T*.

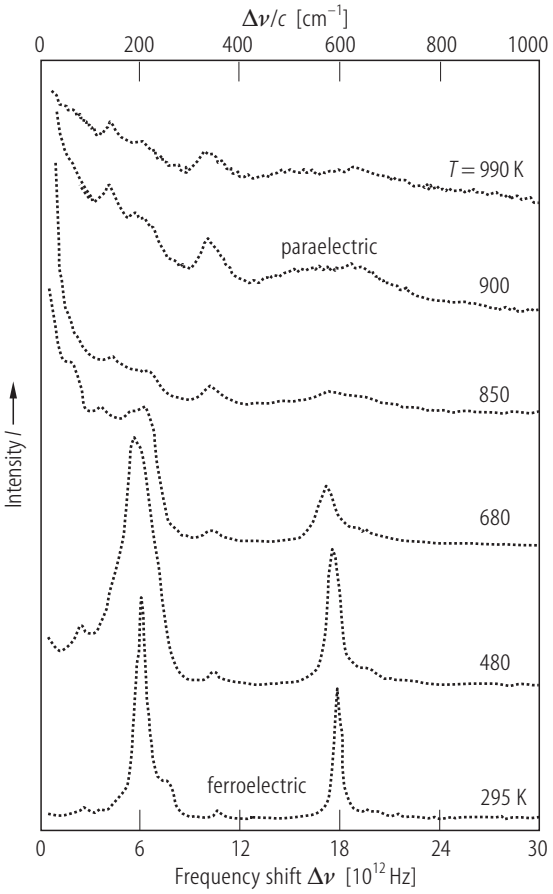

Fig. 2A-2-052. $LiTaO_3$. *Y*(*ZZ*)*X* Raman spectrum of the A_1(TO) (ferroelectric) and A_{1g} (paraelectric) phonons [88Rap]. Parameter: *T*.

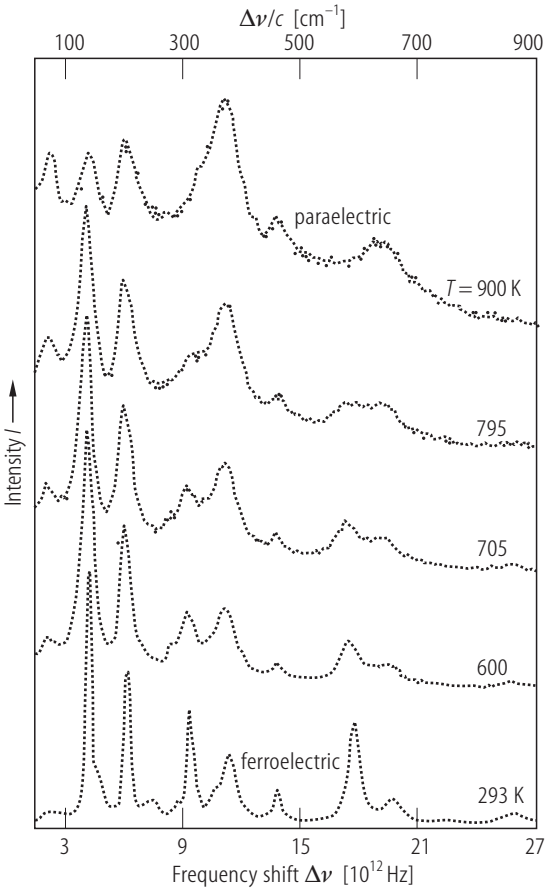

Fig. 2A-2-053. $LiTaO_3$. $Z(XY)Z$ Raman spectrum of E(TO) phonons and oblique phonons in the ferroelectric and E_g phonons in the paraelectric phase [88Rap]. Parameter: *T*.

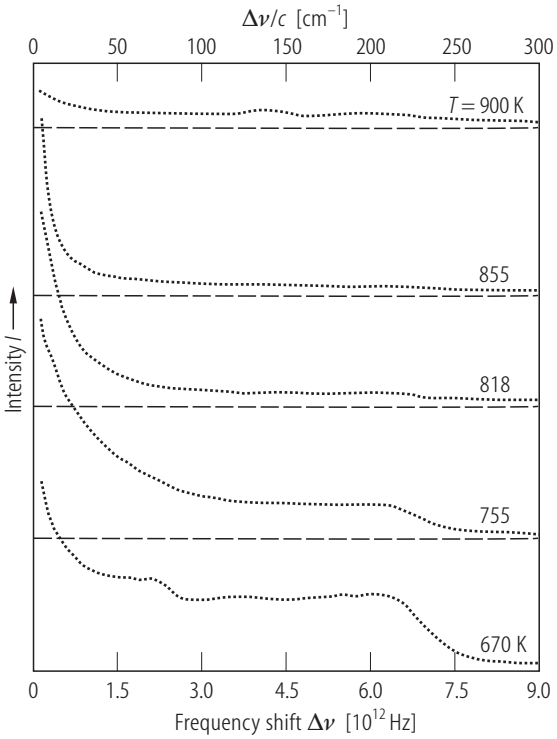

Fig. 2A-2-054. $LiTaO_3$. *Y*(*ZZ*)*X* Raman spectrum [88Rap]. Parameter: *T*.

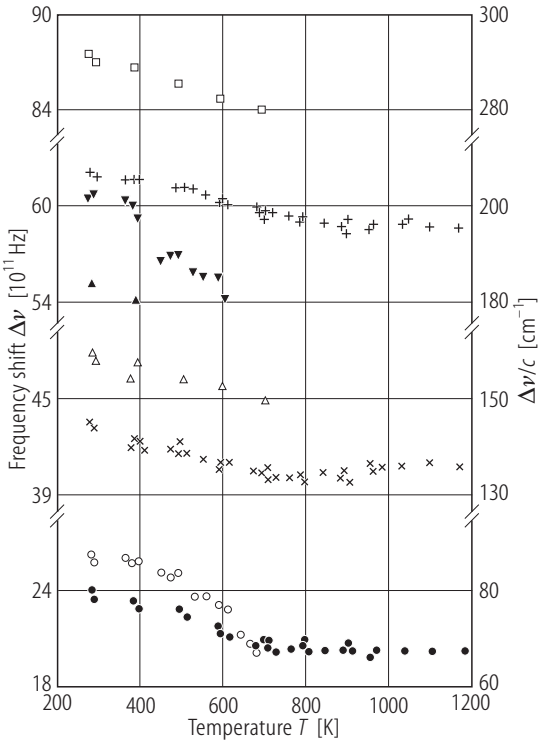

Fig. 2A-2-055. $LiTaO_3$. $\Delta\nu$ vs. T [88Rap]. $\Delta\nu$: Raman shift. Full and open circles: two-phonon (difference) band; crosses: E mode at 142 cm^{-1} in ferroelectric phase (E_g in paraelectric phase); open triangles: oblique phonon at 157 cm^{-1}; full triangles: oblique phonon at 183 cm^{-1}; upside down full triangles: A_1 at 203 cm^{-1}; pluses: $E(E_g)$ at 207 cm^{-1}; open squares: oblique phonon at 293 cm^{-1}. All frequencies refer to room temperature.

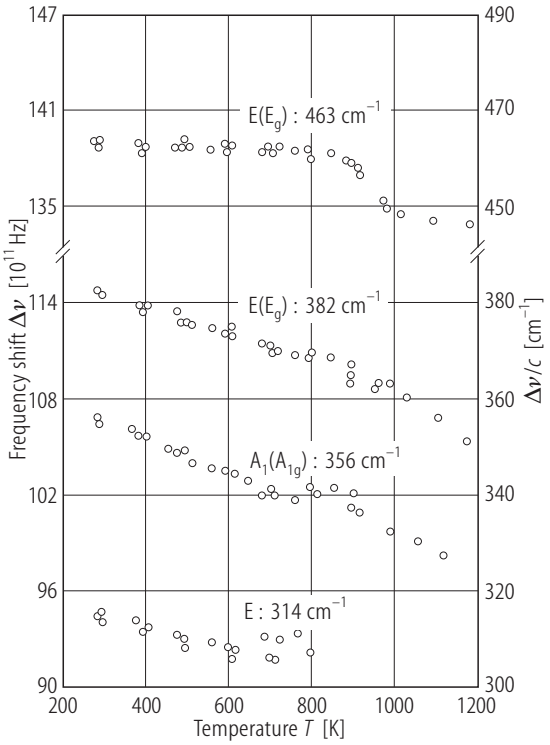

Fig. 2A-2-056. $LiTaO_3$. $\Delta\nu$ vs. T [88Rap]. $\Delta\nu$: Raman shift.

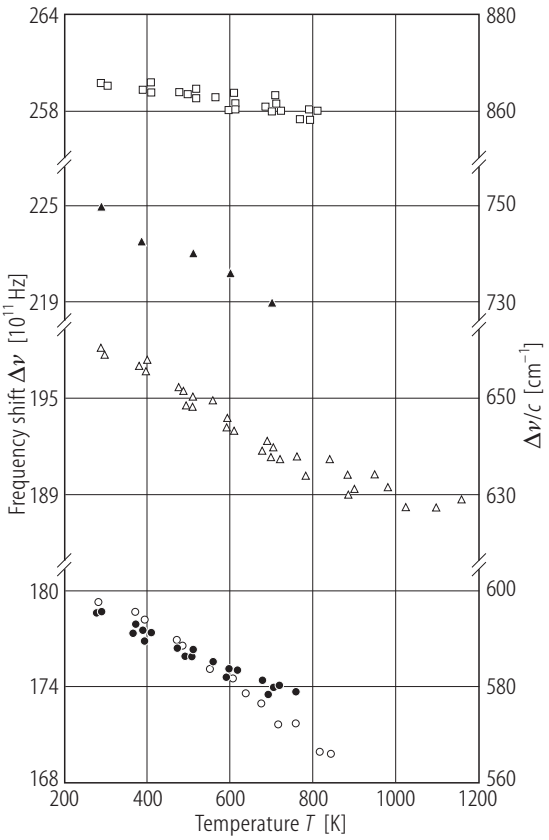

Fig. 2A-2-057. $LiTaO_3$. $\Delta\nu$ vs. T [88Rap]. $\Delta\nu$: Raman shift. Full circles: E mode at 592 cm^{-1}; open circles: A_1 at 597 cm^{-1}; open triangles: two-phonon (summation) band; full triangles: two-phonon (summation) band; open squares: E at 864 cm^{-1}. All frequencies refer to room temperature.

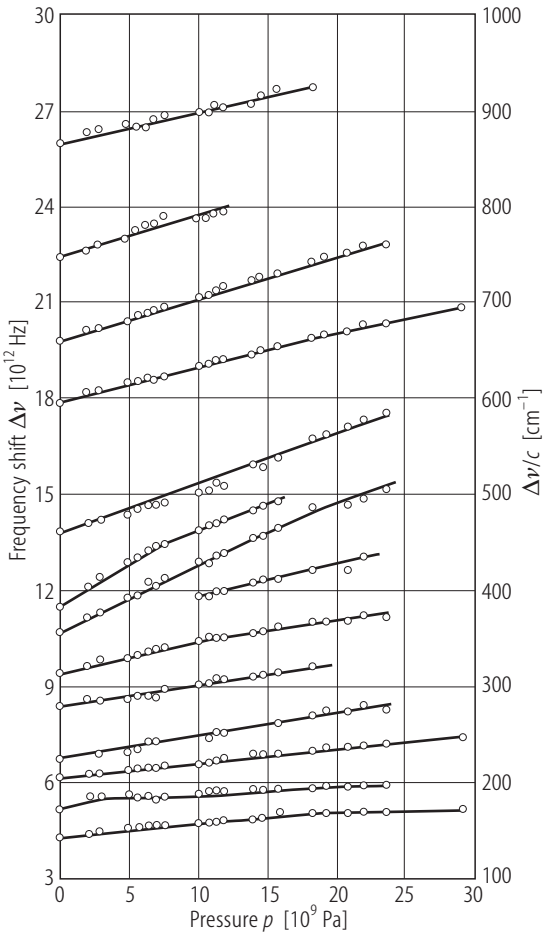

Fig. 2A-2-058. $LiTaO_3$. $\Delta\nu$ vs. p [94Lin]. $\Delta\nu$: Raman shift.

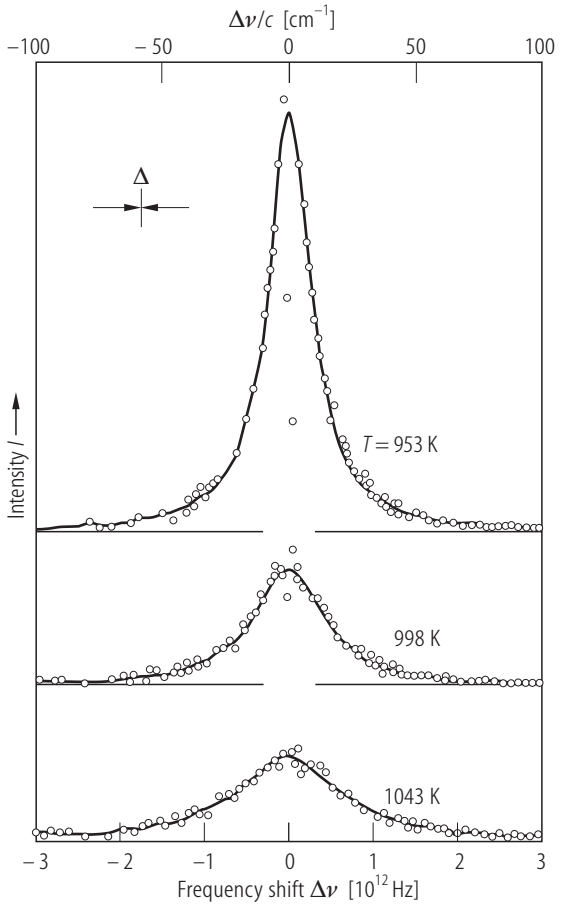

Fig. 2A-2-059. $LiTaO_3$. Central mode of hyper Raman scattering [94Tez]. *I*: scattering intensity. Δ: resolution. Parameter: *T*. *X*(*ZZ*)*Y*.

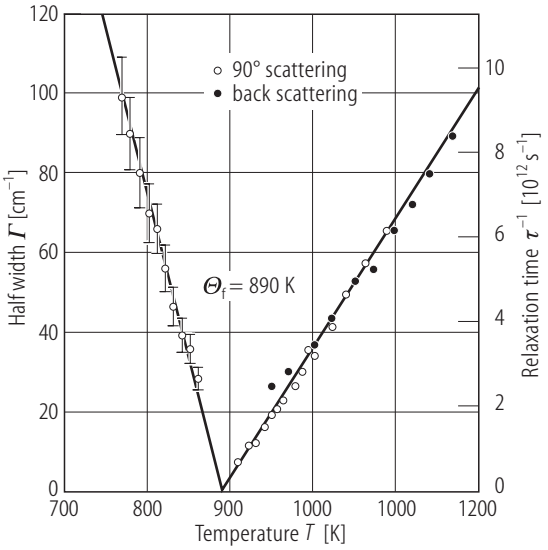

Fig. 2A-2-060. $LiTaO_3$. Γ vs. T [94Tez]. Γ: FWHM of the central mode of hyper Raman scattering. τ: relaxation time.

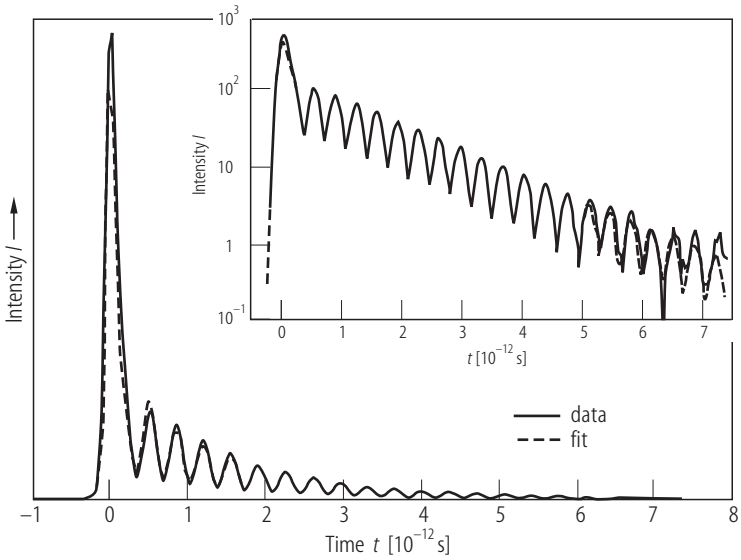

Fig. 2A-2-061. $LiTaO_3$. Real time observation of A_1 polariton at q =1800 cm^{-1} by a femtosecond pulse laser [95Wie]. *I*: scattering intensity. Full line: data; dashed line: fit by a single damped oscillator.

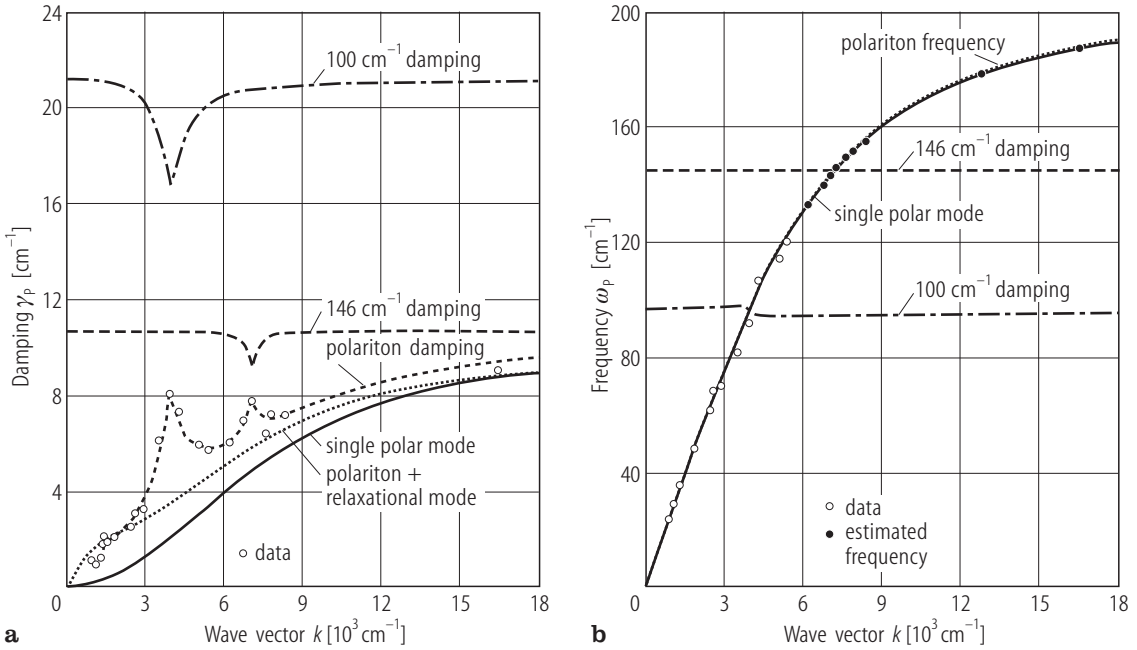

Fig. 2A-2-062. $LiTaO_3$. γ_p, ω_p vs. k [95Wie]. Femtosecond real time observation of A_1 polariton. γ_p: damping constant; ω_p: frequency. $\boldsymbol{k}$: wave number vector.

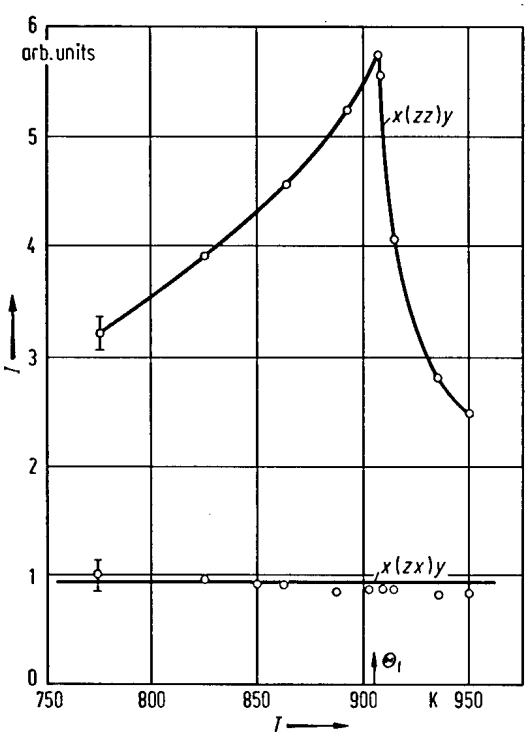

Fig. 2A-2-063. $LiTaO_3$. I vs. T [68Joh]. I: Rayleigh scattering intensity for the scattering geometry of $x(zz)y$ and $z(zx)y$.

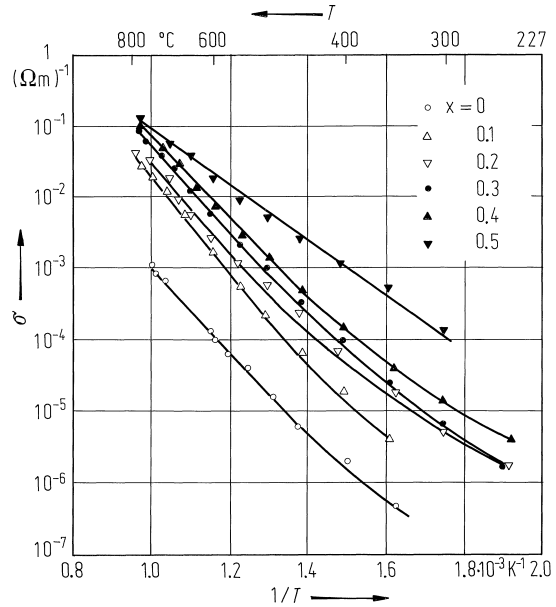

Fig. 2A-2-064. $Li_{1-x}Ta_{1-x}W_xO_3$ (ceramics). σ vs. $1/T$ [85Kaw]. σ: electrical conductivity. Parameter: composition.

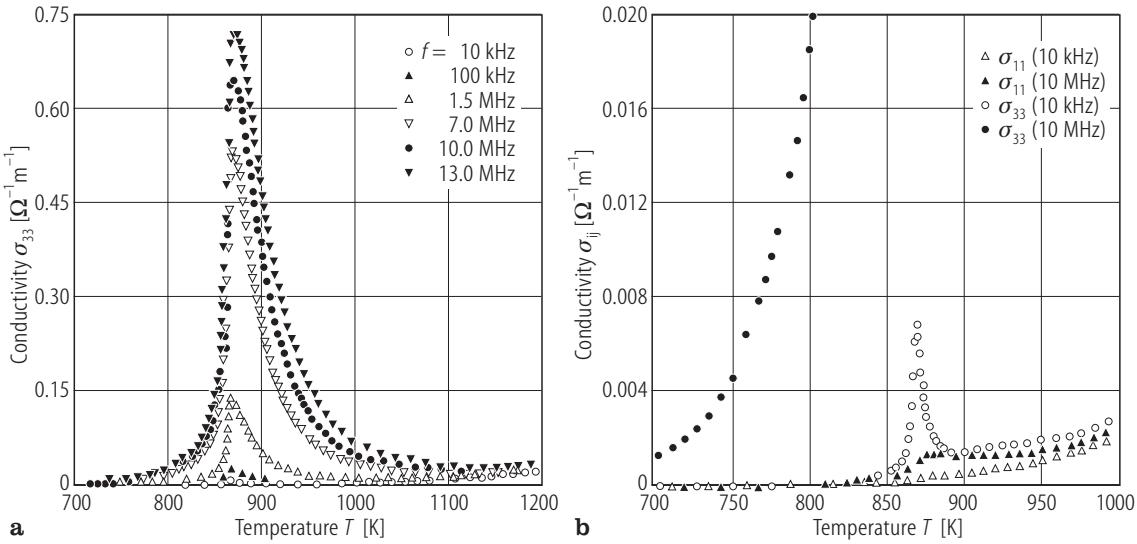

Fig. 2A-2-065. $LiTaO_3$. σ_{11}, σ_{33} vs. T [88Tom]. σ_{11}, σ_{33}: conductivity along the *a*-, *c*-axes, respectively. Parameter: *f*.

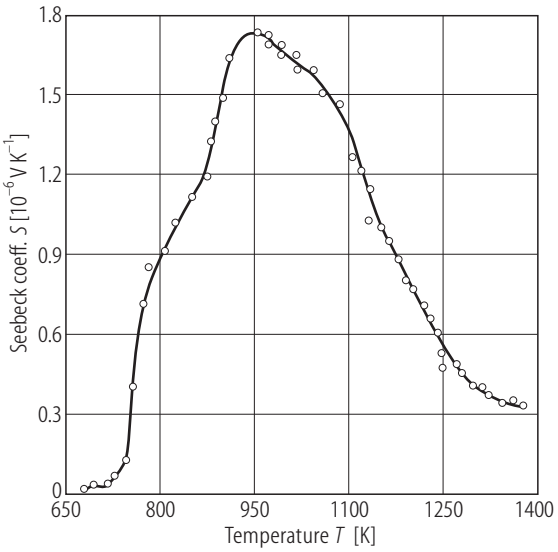

Fig. 2A-2-066. $LiTaO_3$. S vs. T [88Kha]. S: Seebeck coefficient.

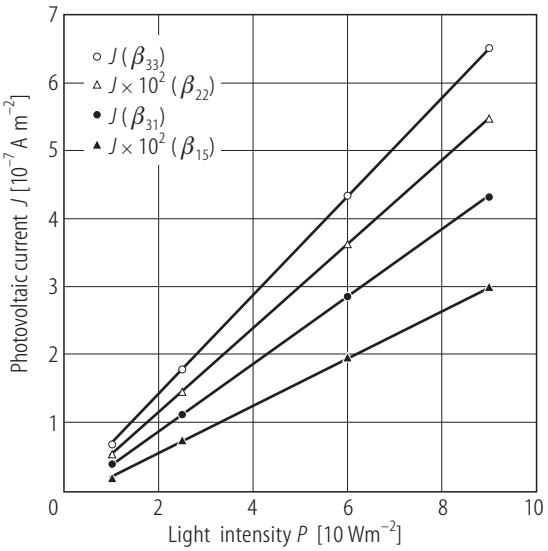

Fig. 2A-2-067. $LiTaO_3$:Fe. J vs. P [92Kar]. J: photovoltaic current; P: light intensity of photon energy 2.6 eV. For definitions of $\beta_{i\lambda}$, see original paper.

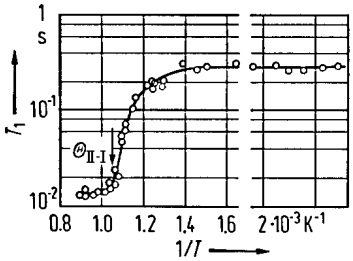

Fig. 2A-2-068. $LiTaO_3$ (powder). T_1 vs. $1/T$ [74Slo]. T_1: spin lattice relaxation time of ^{7}Li. ν_L = 9 MHz.

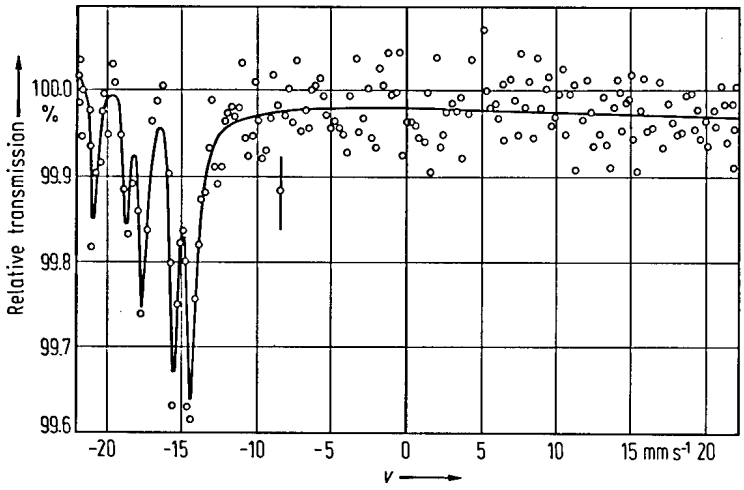

Fig. 2A-2-069. $LiTaO_3$. Mössbauer spectrum at RT [78Wor]. v: $^{181}W(\underline{W})$ source velocity. $^{181}W(\underline{W})$ means ^{181}W in W metal.

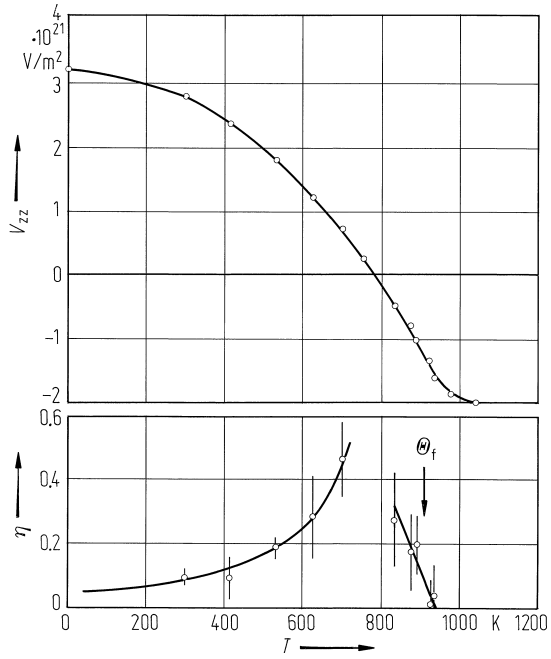

Fig. 2A-2-070. $LiTaO_3$. V_{zz}, η vs. T [81Loh]. V_{zz}: principal component of the electric field gradient tensor at Ta site; η: asymmetry parameter. ^{181}Ta Mössbauer effect.

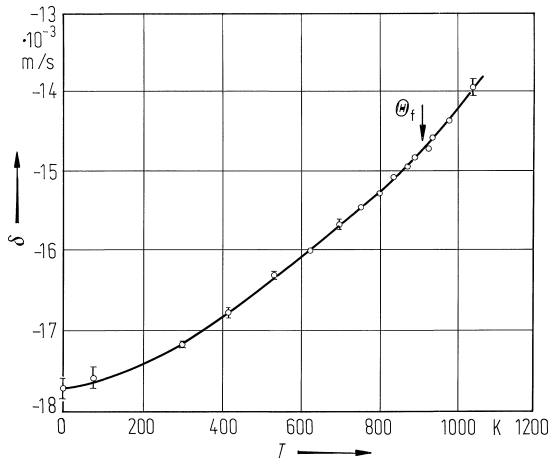

Fig. 2A-2-071. $LiTaO_3$. δ vs. T [81Loh]. δ: line shift of the ^{181} Ta Mössbauer resonance spectrum relative to a W source.

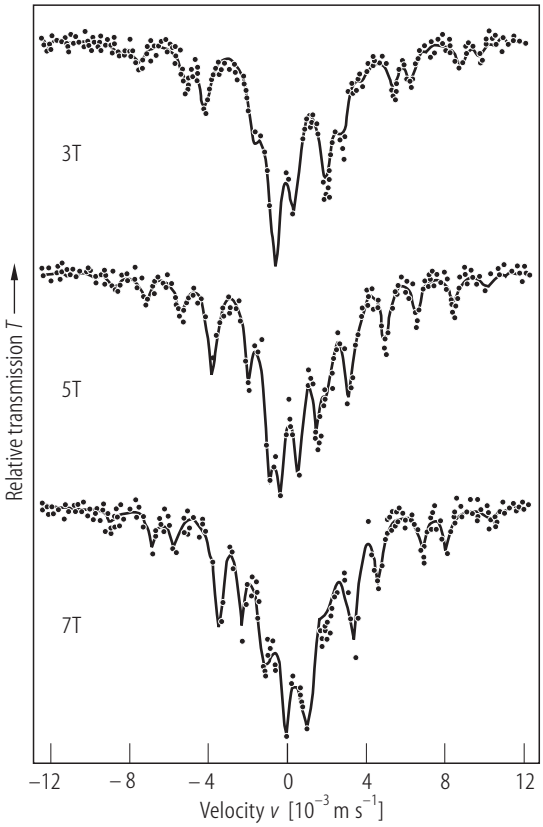

Fig. 2A-2-072. $LiTaO_3$:Fe. ^{57}Fe Mössbauer spectra [90Gie]. Single crystal. $H \parallel c$. Parameter: external magnetic field.

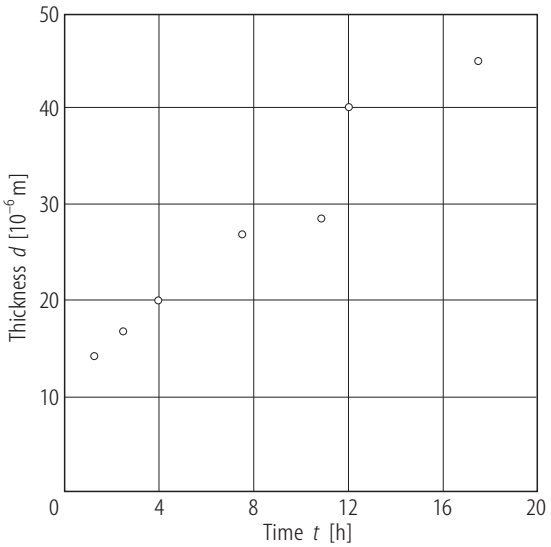

Fig. 2A-2-073. $LiTaO_3$. d vs. t [94Ahl2]. d: single-domain layer thickness on heat treatment at 1100 °C for z-plate. t: heat treatment time.

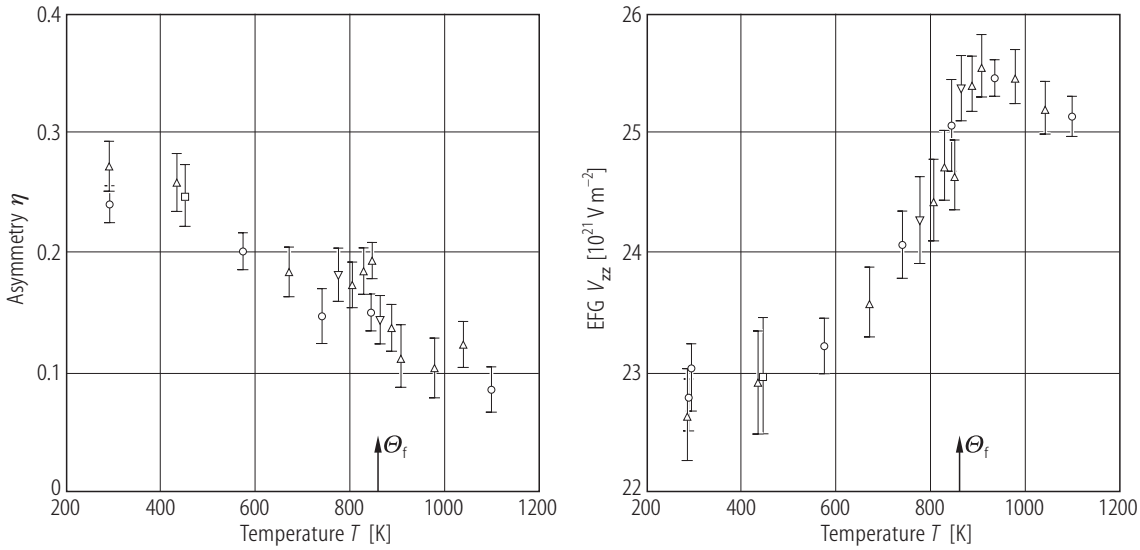

Fig. 2A-2-074. $LiTaO_3$. V_{zz}, η vs. T [91Cat2]. V_{zz}, η: electric field gradient and asymmetry parameter at Li sites determined by $^{181}Hf \rightarrow {}^{181}Ta$ perturbed-angular correlation spectroscopy.

References

49Mat Matthias, B.T., Remeika, J P.: Phys. Rev. **76** (1949) 1886.
54Meg Megaw, H.D.: Acta Crystallogr. **7** (1954) 187.
64Raz Razbirin, B.S.: Fiz. Tverd. Tela **6** (1964) 316; Sov. Phys. Solid State (English Transl.) **6** (1964) 254.
65Bal Ballman, A.A.: J. Am. Ceram. Soc. **48** (1965) 112.
65Bon Bond, W.L.: J. Appl. Phys. **36** (1965) 1674.
65Fed Fedulov, S.A., Shapiro, Z.I., Ladyzhinskii, P.B.: Kristallografiya **10** (1965) 268; Sov. Phys. Crystallogr. (English Transl.) **10** (1965) 218.
66Ash Ashkin, A., Boyd, G.D., Dziedzic, J.M., Smith R.G., Ballman, A.A., Levinstein, J.J., Nassau, K.: Appl. Phys. Lett. **9** (1966) 72
66Len Lenzo, P.V., Turner, E.H., Spencer, E.G., Ballman, A.A.: Appl. Phys. Lett. **8** (1966) 81.
66Lev Levinstein, H.J., Ballman, A.A., Capio, C.D.: J. Appl. Phys. **37** (1966) 4585.
66Tur Turner, E.H.: Paper Th. A13 in Opt. Soc. Am., San Francisco, 1966.
67Abr1 Abrahams, S.C., Bernstein, J.L.: J. Phys. Chem. Solids **28** (1967) 1685.
67Abr2 Abrahams, S.C., Hamilton, W.C., Sequeira, A.: J. Phys. Chem. Solids **28** (1967) 1693.
67Bal Ballman, A.A., Levinstein, H.J., Capio, C.D., Brown, H.: J. Am. Ceram. Soc. **50** (1967) 657.
67Dix Dixon, R.W.: J. Appl. Phys. **38** (1967) 5149.
67Iwa Iwasaki, H., Toyoda, H., Kubota, H.: Jpn. J. Appl. Phys. **6** (1967) 1338.
67Kam Kaminow, I.P., Johnston Jr., W.D.: Phys. Rev. **160** (1967) 519; erratum: **178** (1969) 1528.
67War1 Warner, A.W., Onoe, M., Coquin, G.A.: J. Acoust. Soc. Am. **42** (1967) 1223.
67War2 Warner, A.W., Ballman, A.A.: Proc. IEEE **55** (1967) 450.
68Bur Burns, G., O'Kane, D.F., Title, R.S.: Phys. Rev. **167** (1968) 314.
68Dan Danner, J.C., Ranon, U., Stamires, D.N.: Chem. Phys. Lett. **2** (1968) 605.
68Gla Glass, A.M.: Phys. Rev. **172** (1968) 564.
68Iwa Iwasaki, H., Yamada, T., Niizeki, N., Toyoda, H., Kubota, H.: Jpn. J. Appl. Phys. **7** (1968) 185.
68Joh Johnston Jr., W.D., Kaminow, I.P.: Phys. Rev. **168** (1968) 1045; erratum: **178** (1969) 1528.
68Pet Peterson, G.E., Bridenbaugh, P.M.: J. Chem. Phys. **48** (1968) 3402.
68Wem Wemple, S.H., DiDomenico Jr., M., Camlibel, I.: Appl. Phys. Lett. **12** (1968) 209.
68Yam1 Yamada, T., Niizeki, N., Toyoda, H.: Jpn. J. Appl. Phys. **7** (1968) 298.
68Yam2 Yamada, T., Niizeki, N., Toyoda, H.: Jpn. J. Appl. Phys. **7** (1968) 292.
69Bec Bechmann, R., Hearmon, R.F.S., Kurtz, S.K.: Landolt-Börnstein, New Series, Group III, Vol. 2: Elastic, Piezoelectric, Piezooptic, Electrooptic Constants, and Nonlinear Dielectric Susceptibilities of Crystals, Hellwege, K.-H., Hellwege, A.M. (eds.), Berlin, Heidelberg, New York: Springer, 1969.
69Gla Glass, A.M.: J. Chem. Phys. **50** (1969) 1501.
69Val Valitova, N.R., Goncharov, K.V., Krasil'nikov, V.A., Palamarchuk, I.V., Salamatin, E.P.: Fiz. Tverd. Tela **11** (1969) 3639; Sov. Phys. Solid State (English Transl.) **11** (1970) 3055.
69Yam Yamada, T., Iwasaki, H., Niizeki, N.: Jpn. J. Appl. Phys. **8** (1969) 1127.
70Bar1 Barns, R.L., Carruthers, J.R.: J. Appl. Crystallogr. **3** (1970) 395.
70Bar2 Barker Jr., A.S., Ballman, A.A., Ditzenberger, J.A.: Phys. Rev. B **2** (1970) 4233.
70Mil Miller, R.C., Nordland, W.A.: Phys. Rev. B **2** (1970) 4896.
70Saw Sawamoto, K., Ashida, T., Omachi, Y., Uno, T.: J. Phys. Soc. Jpn **28**, Suppl. (1970) 309.
70Wor Worley, J.C., Smith, A.B., Kestingian, M.: J. Phys. Chem. Solids **31** (1970) 1857.
71Fuj Fujino, Y., Tsuya, H., Sugibuchi, K.: Ferroelectrics **2** (1971) 113.
71Kha Khashkhozhev, Z.M., Lemanov, V.V., Pisarev, R.V.: Izv. Akad. Nauk SSSR, Ser. Fiz. **35** (1971) 987; Bull. Acad. Sci. USSR, Phys. Ser. (English Transl.) **35** (1971) 911.
71Miy Miyazawa, S., Iwasaki, H.: J. Cryst. Growth **10** (1971) 276.
71Smi Smith, R.T., Welsh, F.S.: J. Appl. Phys. **42** (1971) 2219.

72Onu Onuki, K., Uchida, N., Saku, T.: J. Opt. Soc. Am. **62** (1972) 1030.
72Sch1 Schulz, M.B., Holland, M.G.: IEEE Trans. Sonics Ultrason. SU-**19** (1972) 381.
72Sch2 Schulz, M.B., Matsinger, J.H.: Appl. Phys. Lett. **20** (1972) 367.
72Zve Zverev, G.M., Levchuk, E.A., Pashkov, V.A., Poryadin, Yu.D.: Zh. Eksp. Teor. Fiz. **62** (1972) 307; Sov. Phys. JETP (English Transl.) **35** (1972) 165.
73Abr Abrahams, S.C., Buehler, E., Hamilton, W.C., Laplaca, S.J.: J. Phys. Chem. Solids **34** (1973) 521.
73Gia Gia Russo, D.P., Kumar, C.S.: Appl. Phys. Lett. **23** (1973) 229.
73Kam Kaminow, I.P., Carruthers, J.R.: Appl. Phys. Lett. **22** (1973) 326.
73Sza Szabo, T.L., Slobodnik Jr., A.J.: IEEE Trans. Sonics Ultrason. SU-**20** (1973) 240.
74Ham Hammer, J.M., Phillips, W.: Appl. Phys. Lett. **24** (1974) 545.
74Nod Noda, J., Saku, T., Uchida, N.: Appl. Phys. Lett. **25** (1974) 308.
74Slo Slotfeldt-Ellingsen, D., Pedersen, B.: Phys. Status Solidi (a) **24** (1974) 191.
75Bee Beerman, H.P.: Infrared Phys. **15** (1975) 225.
75Par Parker, T.E., Schulz, M.B.: Appl. Phys. Lett. **26** (1975) 75.
75Tea Teague, J.R., Rice, R.R., Gerson, R.: J. Appl. Phys. **46** (1975) 2864.
75Tie Tien, P.K., Ballman, A.A.: J. Vacuum Sci. Technol. **12** (1975) 892.
76Ava Avakyants, L.P., Kiselev, D.F., Shchitov, N.N.: Fiz. Tverd. Tela **18** (1976) 2129; Sov. Phys. Solid State (English Transl.) **18** (1976) 1242.
76Bur Burgess, J.W., Hales, M.C.: Proc. Inst. Electr. Eng. **123** (1976) 499.
76Gra Graham, R.A.: Ferroelectrics **10** (1976) 65.
76Pen1 Penna, A.F., Chaves, A., Andrade, P., Da, R., Porto, S.P.S.: Phys. Rev. B **13** (1976) 4907.
76Pen2 Penna, A.F., Porto, S.P.S., Chaves, A.S.: Proc. Int. Conf. Light Scattering Solids, 3 rd, Campinas, Brazil, July 1975, New York: Flammarion Sciences or John Wiley & Sons, Inc., 1976, p. 890.
76Pen3 Penna, A.F., Chaves, A., Porto, S.P.S.: Solid State Commun. **19** (1976) 491.
77Dub Dubbers, D., Dörr, K., Ackermann, H., Fujara, F., Grupp, H., Grupp, M., Heitjans, P., Körblein, A., Stöckmann, H.-J.: Z. Phys. A **282** (1977) 243.
77Gla Glass, A.M., Lines, M.E., Nassau, K., Shiever, J.W.: Appl. Phys. Lett. **31** (1977) 249.
77Hir Hirano, H., Fukuda, T., Matsumura, S., Takahashi, S.: Proc. First Meeting on Ferroelectric Materials and Their Applications, Kyoto, Tanaka, T. (chairman), Kyoto: Department of Electronics, Kyoto University, 1977, p. 81.
77Lin Lines, M.E., Glass, A.M.: Phys. Rev. Lett. **39** (1977) 1362.
78Wor Wortmann, G., Trollmann, G., Heidemann, A., Kalvius, G.M.: Hyperfine Interact. **4** (1978) 610.
80Bha Bhalla, A.S., Newnham, R.E.: Phys. Status Solidi (a) **58** (1980) K19.
80Roz Rozenman, G.I., Rez, I.S., Chepelev, Yu.L., Angert, N.B., Zhashkov, A.A.: Fiz. Tverd. Tela **22** (1980) 3466; Sov. Phys. Solid State (English Transl.) **22** (1980) 2032.
80Ser Servoin, J.L., Gervais, F.: Ferroelectrics **25** (1980) 609.
81Cor Cordero-Montalvo, C., Vedam, K.: J. Appl. Phys. **52** (1981) 944.
81Ina Inaba, R., Wasa, K.: Jpn. J. Appl. Phys. **20**, Suppl. 20-3 (1981) 153.
81Loh Löhnert, M., Kaindl, G., Wortmann, G., Salomon, D.: Phys. Rev. Lett. **47** (1981) 194.
81Rit Ritz, V.H., Bermudez, V.M.: Phys. Rev. B **24** (1981) 5559.
82Fuj Fujimoto, I.: Acta Crystallogr., Sect. A **38** (1982) 337.
82Lin Lin, P.J., Bursill, L.A.: Philos. Mag. A **45** (1982) 911.
82Tom Tomeno, I.: J. Phys. Soc. Jpn. **51** (1982) 2891.
82Yas1 Yasuami, S., Fukuda, T.: J. Cryst. Growth **57** (1982) 570.
82Yas2 Yasuhara, Y., Yamaji, N., Kurokawa, T., Takahashi, K.: IEEE Trans. Consum. Electron., CE-**28** (1982) 475.
83Ahn Ahn, B.H., Clark III, W.W., Schurtz II, R.R., Bates, C.D.: J. Appl. Phys. **54** (1983) 1251.
83Bro Brody, P.S., Sattler, J.P., Simonis, G.J.: Ferroelectrics **50** (1983) 319.

83Mam Mamedov, A.M.: Izv. Akad. Nauk SSSR, Ser. Fiz. **47** (1983) 660; Bull. Acad. Sci. USSR, Phys. Ser. (English Transl.) **47** (1983) 34.
83Spi Spillman Jr., W.B., Sanford, N.A., Soref, R.A.: Opt. Lett. **8** (1983) 497.
83Tor Torii, Y., Sekiya, T., Yamamoto, T., Kobayashi, K., Abe, Y.: Mater. Res. Bull. **18** (1983) 1569.
84Yam Yamada, K., Omi, T., Matsumura, S., Nishimura, T.: Proc. IEEE Ultrasonic Symp., 1984, 243.
85Bor Borisov, V.N., Pereverzeva, L.P: Fiz. Tverd. Tela **27** (1985) 3112; Sov. Phys. Solid State (English Transl.) **27** (1985) 1869.
85Hir Hirano, H.: Jpn. J. Appl. Phys. **24**, Suppl. 24-2 (1985) 31.
85Kaw Kawakami, S., Tsuzuki, A., Sekiya, T., Ishikuro, T., Masuda, M., Torii, Y.: Mater. Res. Bull. **20** (1985) 1435.
85Kha Khachatryan, R.M., Petrosyan, A.K., Sharoyan, É.G.: Fiz. Tverd. Tela **27** (1985) 2713; Sov. Phys. Solid State (English Transl.) **27** (1985) 1626.
85Sen Senegas, J., Zriouil, M.: J. Solid State Chem. **58** (1985) 137.
86Hay Haycock, P.W., Townsend, P.D.: Appl. Phys. Lett. **48** (1986) 698.
86Jay Jayaraman, A., Ballman, A.A.: J. Appl. Phys. **60** (1986) 1208.
86Pri Prieto, C., Arizmendi, L., Gonzalo, J.A., Jaque, F., Agullo-Lopez, F.: Phys. Rev. B **34** (1986) 7396.
86Red Red'kin, B.S., Satunkin, G.A., Kurlov, V.N., Tatarchenko, V.A.: Rost Krist. **15** (1986) 210; Growth Cryst. (English Transl.) **15** (1988) 223.
86Zha Zhang, M.S., Scott, J.F.: Phys. Rev. B **34** (1986) 1880.
87Don Donnerberg, H.J., Schirmer, O.F.: Solid State Commun. **63** (1987) 29.
87Hua Huanosta, A., West, A.R.: J. Appl. Phys. **61** (1987) 5386.
87Kan Kanata, T., Kobayashi, Y., Kubota, K.: J. Appl. Phys. **62** (1987) 2989.
87Pri Prieto, C., Gonzalo, J.A.: Solid State Commun. **61** (1987) 437.
87Vor Voron'ko, Yu.K., Kudryavtsev, A.B., Osiko, V.V., Sobol', A.A., Sorokin, E.V.: Fiz. Tverd. Tela **29** (1987) 1348; Sov. Phys. Solid State (English Transl.) **29** (1987) 771.
87Yan Yang, X.C., Lan, G.X., Li, B., Wang, H.F.: Phys. Status Solidi (b) **141** (1987) 287.
88Kha Khachaturyan, O.A., Gabrielyan, A.I., Kolesnik, S.P.: Fiz. Tverd. Tela **30** (1988) 888; Sov. Phys. Solid State (English Transl.) **30** (1988) 514.
88Rap Raptis, C.: Phys. Rev. B **38** (1988) 10007; erratum: **40** (1989) 3399.
88Rav Ravez, J., Puyoo-Castaings, N., Duboudin, F.: Ferroelectrics **81** (1988) 313.
88Tom Tomeno, I., Matsumura, S.: Phys. Rev. B **38** (1988) 606.
88Yoo Yoon, D.W., Eknoyan, O.: J. Lightwave Technol. **6** (1988) 877.
89Gan Ganshin, V.A., Korkishko, Yu.N., Morozova, T.V., Saraikin, V.V.: Phys. Status Solidi (a) **114** (1989) 457.
89Sin Sinclair, D.C., West, A.R.: Phys. Rev. B **39** (1989) 13486.
89Sot Söthe, H., Rowan, L.G., Spaeth, J.M.: J. Phys. Condens. Matter **1** (1989) 3591.
89YeZ Ye, Z.G., von der Muhl, R., Ravez, J.: Mater. Sci. Eng. B **5** (1989) 47.
90And Andler, G., Engelmann, H., Dezsi, I., Gonser, U.: Hyperfine Interact. **55** (1990) 1121.
90Gan Ganshin, V.A., Korkishko, Yu.N.: Phys. Status Solidi (a) **119** (1990) 11.
90Gie Giesse, E., Gruber, W., Leupold, O., Molnár, B., Nagy, D.L., Ritter, G.: Hyperfine Interact. **56** (1990) 1519.
90InH In, H.B., von der Muhll, R., Ye, Z.G., Ravez, J.: Proc. Seventh International Symposium on the Applications of Ferroelectrics, June 1990, Urbana-Champaign, IL, Krupanidhi, S.B., Kurtz, S.K. (eds.), New York: The Institute of Electrical and Electronics Engineers, Inc., 1990,
p. 367.
90Jea1 Jean, J.H.: J. Mater. Sci. **25** (1990) 2267.
90Jea2 Jean, J.H.: J. Mater. Sci. **25** (1990) 859.

90Leu Leupóld, O., Billenstein, M., Giesse, E., Gruber, W., Molnár, B., Nagy, D.L., Ritter, G., Röhlich, U.: Hyperfine Interact. **56** (1990) 1539.

90YeZ Ye, Z.G., Von der Muhll, R., Ravez, J.: Ferroelectrics **108** (1990) 177.

90Zha Zhang, J.X., Zeng, W.G., Luo, Y.L., Siu, G.G., Stokes, M.J., Meng, X.L., Xu, B.C.: J. Phys. Condens. Matter **2** (1990) 4579.

91Bob Bobrov, Yu.A., Ganshin, V.A., Ivanov, V.Sh., Korkishko, Yu.N., Morozova, T.V.: Phys. Status Solidi (a) **123** (1991) 317.

91Cat1 Catlow, C.R.A., Chadwick, A.V., Cole, M., Tomlinson, S.M.: Radiat. Eff. Defects Solids **119-121** (1991) 565.

91Cat2 Catchen, G.L., Spaar, D.M.: Phys. Rev. B **44** (1991) 12137.

91Chi Chiou, B.S., Lin, T.Y., Duh, J.G.: Mater. Chem. Phys. **28** (1991) 51.

91Kus Kushibiki, J., Takahashi, H., Kobayashi, T., Chubachi, N.: Appl. Phys. Lett. **58** (1991) 893.

91Miz1 Mizuuchi, K., Yamamoto, K., Taniuchi, T.: Appl. Phys. Lett. **58** (1991) 2732.

91Miz2 Mizuuchi, K., Yamamoto, K., Taniuchi, T.: Appl. Phys. Lett. **59** (1991) 1538.

91Mur Murota, M. , Shimizu, Y.: Jpn. J. Appl. Phys. **30**, Suppl. 30-1 (1991) 156.

91Nov Novikov, V.N., Novik, V.K., Esengaliev, A.B., Gavrilova, N.D.: Ferroelectrics **118** (1991) 59.

91Sai Saito, Y., Shiosaki, T.: Jpn. J. Appl. Phys. **30** (1991) 2204.

91Yam Yamamoto, K., Mizuuchi, K., Takeshige, K., Sasai, Y., Taniuchi, T.: J. Appl. Phys. **70** (1991) 1947.

92Bak Bakker, H.J., Hunsche, S., Kurz, H.: Phys. Rev. Lett. **69** (1992) 2823.

92Kar Karabekian, S.I., Odoulov, S.G.: Phys. Status Solidi (b) **169** (1992) 529.

92Mae Maeda, M., Suzuki, I., Sakiyama, K.: Jpn. J. Appl. Phys. **31** (1992) 3229.

92Mak Makio, S., Nitanda, F., Ito, K., Sato, M.: Appl. Phys. Lett. **61** (1992) 3077.

92McW McWright Howerton, M., Burns, W.K.: J. Lightwave Technol. **10** (1992) 142.

92Miz1 Mizuuchi, K., Yamamoto, K.: J. Appl. Phys. **72** (1992) 5061.

92Miz2 Mizuuchi, K., Yamamoto, K.: Appl. Phys. Lett. **60** (1992) 1283.

92Sai Saito, Y., Hori, S., Shiosaki, T.: Ceramic Transactions, Vol. 25. Ferroelectric Films, Proceedings of the Symposium, Cincinnati, OH, April-May 1991, Bhalla, A.S., Nair, K.M. (eds.), Westerville: The American Ceramic Society, Inc., 1992, p. 293.

92Sha Shaldin, Y.V.: Opt. Spektrosk. **72** (1992) 913; Opt. Spectrosc. (English Transl.) **72** (1992) 492.

92Yam1 Yamamoto, K., Mizuuchi, K., Taniuchi, T.: Jpn. J. Appl. Phys. **31** (1992) 1059.

92Yam2 Yamamoto, K., Mizuuchi, K.: IEEE Photonics Technol. Lett. **4** (1992) 435.

92Yam3 Yamamoto, K., Mizuuchi, K., Taniuchi, T.: IEEE J. Quantum Electron. **28** (1992) 1909.

92Yuh Yuhara, T., Tada, K., Li, Y.S.: J. Appl. Phys. **71** (1992) 3966.

93Dei Deis, T.A., Phulé, P.P.: Mater. Res. Bull. **28** (1993) 167.

93Hun Hung, L.S., Agostinelli, J.A., Mir, J.M., Zheng, L.R.: Appl. Phys. Lett. **62** (1993) 3071.

93Shi Shibata, Y., Kaya, K., Akashi, K., Kanai, M., Kawai, T., Kawai, S.: Jpn. J. Appl. Phys. **32** (1993) L745.

93Tou Tourlog, A., Nakamura, K.: Jpn. J. Appl. Phys. **32** (1993) 4370.

93Wan Wang, X.S., Gao, J.X., Tang, N.A.: Ferroelectr. Lett. **15** (1993) 49.

93Xie Xie, H.Y., Raj, R.: Appl. Phys. Lett. **63** (1993) 3146.

94Ahl1 Åhlfeldt, H.: J. Appl. Phys. **76** (1994) 3255.

94Ahl2 Åhlfeldt, H.: Appl. Phys. Lett. **64** (1994) 3213.

94Gup Gupta, M.C., Kozlovsky, W., Nutt, A.C.G.: Appl. Phys. Lett. **64** (1994) 3210.

94Len Leng, S.Y., Yu, Y.S.: Phys. Status Solidi (a) **143** (1994) 431.

94Lin Lin, Y.K., Lan, G.X., Wang, H.F.: Solid State Commun. **91** (1994) 879.

94Miz1 Mizuuchi, K., Yamamoto, K., Sato, H.: J. Appl. Phys. **75** (1994) 1311.

94Miz2 Mizuuchi, K., Yamamoto, K.: Appl. Opt. **33** (1994) 1812.

94Oka Okano, Y., Tsuji, Y., Yoon, D.H., Hoshikawa, K., Fukuda, T.: J. Cryst. Growth **141** (1994) 383.

94Rav Ravez, J., Joo, G.T., Dong, M., Reau, J.M.: Phys. Status Solidi (a) **146** (1994) K71.

94Tak Taki, K., Shimizu, Y.: Jpn. J. Appl. Phys. **33** (1994) 2976.
94Tez Tezuka, Y., Shin, S., Ishigame, M.: Phys. Rev. B **49** (1994) 9312.
94Thi Thiemann, O., Donnerberg, H., Wohlecke, M., Schirmer, O.F.: Phys. Rev. B **49** (1994) 5845.
94Tom Tomita, Y., Sugimoto, M., Eda, K., Okano, T.: Jpn. J. Appl. Phys. **33** (1994) L1542.
94WuX1 Wu, X.L., Zhang, M.S., Chen, Q., Zou, Q., Geng, Z.H., Feng, D.: Acta Phys. Sin. **3** (1994) 493.
94WuX2 Wu, X.L., Zhang, M.S., Chen, X.Y., Meng, X.K., Feng, D.: Appl. Phys. Lett. **65** (1994) 1088.
95Wie Wiederrecht, G.P., Dougherty, T.P., Dhar, L., Nelson, K.A., Leaird, D.E., Weiner, A.M.: Phys. Rev. B **51** (1995) 916.
95WuX Wu, X.L., Zhang, M.S., Yan, F., Feng, D.: Solid State Commun. **93** (1995) 131.